CHARACTERIZATION OF DEPOSITED LAYER AFTER ELECTRICAL DISCHARGE COATING (EDC) PROCESS

NORHAZERATUL BINTI MOHAMMAD ZAINUDIN

UNIVERSITI TEKNIKAL MALAYSIA MELAKA

2021

CHARACTERIZATION OF DEPOSITED LAYER AFTER ELECTRICAL DISCHARGE COATING (EDC) PROCESS

This report is submitted in accordance with requirement of the Universiti Teknikal Malaysia Melaka (UTeM) for Bachelor Degree of Manufacturing Engineering (Hons.)

by

NORHAZERATUL BINTI MOHAMMAD ZAINUDIN

FACULTY OF MANUFACTURING ENGINEERING

2021

DECLARATION

I hereby, declared this report entitled "Characterization of Deposited Layer After Electrical Discharge Coating (EDC) Process" is the result of my own research except as cited in references.

Signature   : ....*hazera*.........................
Author's Name   : NORHAZERATUL BINTI MOHAMMAD ZAINUDIN
Date   : 8 Februari 2021

APPROVAL

This report is submitted to the Faculty of Manufacturing Engineering of Universiti Teknikal Malaysia Melaka as a partial fulfilment of the requirement for Degree of Manufacturing Engineering (Hons). The member of the supervisory committee is as follow:

ASSOC. PROF. DR. LIEW PAY JUN
Faculty of Manufacturing Engineerir
Universiti Teknikal Malaysia Melaka

……………………….....………………………
(Prof. Madya Dr Liew Pay Jun)

ABSTRAK

Dalam industri, aluminium siri 6000 digunakan secara meluas dalam pembuatan mesin pengacuanan kerana sifatnya yang unik. Ianya mempunyai nisbah kekuatan dan berat yang hebat, pengalir elektrik yang baik, tahan pada hakisan dan kerosakan dan juga mudah diubah bentuk. Walaupun aluminium mempunyai ketahanan daripada hakisan dan kerosakan, dalam beberapa jangka masa, kualitinya akan menurun. Dalam kajian ini, pengubahsuaian permukaan aluminium 6061 telahpun dilakukan dengan menggunakan Lapisan Pelepasan Electrik (EDC) dengan penggantungan serbuk atau Permesinan Campuran Serbuk Lepasan Elektrik (PMEDM). Nilai purata saiz zarah dan morfologi serbuk tungsten (W) dicirikan dengan menggunakan Scanning Electron Microscopy (SEM) dan kesan arus puncak (Ip) serta nadi tepat waktu (T_{ON}) pada ketebalan lapisan dikaji selepas proses EDC. Serbuk W telah digunakan sebagai bahan tambahan dalam minyak tanah dengan parameter Ip yang dipelbagaikan pada 3A dan 4A dan T_{ON} pada 150 µs, 200 µs dan 250 µs, manakala parameter yang lainnya seperti voltan yang dilepaskan (V), kepekatan serbuk (g/L) dan waktu permesinan adalah tetap. Mesin Sodick AQ35L die sinker digunakan untuk menjalankan proses EDC. Batang elektrod digilap dan dibersihkan terlebih dahulu untuk mendapatkn permukaan yang rata pada pangkalnya dan penyediaan campuran bahan bendalir sebelum eksperimen dijalankan. Setelah eksperimen siap dijalankan, ketebalan lapisan dikaji. Keputusan yang diperolehi menunjukkan purata saiz serbuk adalah pada 1.29 µm dan mempunyai bentuk yang tidak tetap. Selain daripada itu, lapisan yang paling nipis ditemui pada 3A, 150 µs dengan purata ketebalan adalah sebanyak 6.724 µm, manakala lapisan yang paling tebal dengan purata ketebalan sebanyak 17.239 µm ditemui pada parameter 4A, 250 µs. Kesimpulannya, nilai Ip yang tinggi dan jangka masa T_{ON} yang panjang meningkatkan ketebalan lapisan.

ABSTRACT

In industry, aluminium 6000 series is widely used for fabrication of mold and die due to its unique characteristic. It has a great strength-to-weight ratio, good conductivity, resistance to wear and corrosion and also easy to form. Although aluminum is resistance to corrosion and wear, after some duration of time, it will degrade. In this research, surface modification of aluminium 6061 was carried out by using electrical discharge coating (EDC) with powder suspension or powder mixed electrical discharge machining (PMEDM). The average particle size and morphology of tungsten (W) powder was characterized by using Scanning Electron Microscopy (SEM) and the effect of peak current (Ip) and pulse on time (Ton) on the coating layer thickness were investigated after the EDC process. W powder was used as an additive in the kerosene oil and the parameters of Ip were varied at 3A and 4A and Ton at 150μs, 200 μs and 250 μs, while the other parameters such as discharge voltage (V) and powder concentration (g/L) and machining time remains constant. Sodick AQ35L die sinker machine was used to run the EDC experiment. Electrode was polished and clean first to get a flat surface on the base and the preparation of mixture was done before the experiment run. After the experiment, thickness of coating layer was investigated. The result shows that the average particle size of W powder is 1.29 μm and in irregular shape. On the other hand, thinnest coating layer was observed at 3A, 150 μs with the average value 6.724 μm, while thickest coating layer with the average value 17.239 μm was observed at parameter 4A and 250 μs. As a conclusion, a high value of Ip current and longer duration of Ton increased the thickness of coating layer.

DEDICATION

I would like to dedicate my work to my beloved husband, Mohd Hisyamuddin Bin Mohd Zin, my lovely father and mother Mohammad Zainudin Bin Abdul Kadir and Tamah Binti Lazim for their support, understanding and encouragement along the journey to finish this report.

Not forgotting my sweet little boy, Muhammad Asyraf Hardy Bin Mohd Hisyamuddin for always make my days bright and happy. Although there is a lot of obstacle and need to face a lot of pressure, their existence in my life make me realize that family is always the best listener and du'a from all of them is the bridge for my to success.

Thank You So Much & Love You All Forever

ACKNOWLEDGEMENT

In the name of ALLAH, the most gracious, the most merciful, with the highest praise to Allah that I manage to complete this final year project successfully without difficulty.

Thank you to my respected supervisor, Professor Madya Dr Liew Pay Jun for the great mentoring that was given to me throughout the project. Besides that, I would like to express my gratitude to my beloved supervisor for kind supervision, advice and guidance as well as exposing me with meaningful experiences throughout the study.

Last but not least, I would like to give a special thanks to my best friends who gave me much motivation and cooperation in completing this report especially to Amyliana binti Mahasaan, Nudra Syafina binti Yazid that always give me moral support and Yap Ching Yee that always give me useful advice and many information for my research. Thanks for the great friendship.

Finally, I would like to thank everybody who was important to this PSM report, as well as expressing my apology that I could not mention personally each one of you.

TABLE OF CONTENTS

UNIVERSITI TEKNIKAL MALAYSIA MELAKA

LIST OF TABLE

LIST OF FIGURES

LIST OF EQUATION

3.1   Concentration of mixture (g/L) = $\dfrac{\text{Powder Weight (g)}}{\text{Volume of dielectric Fluid (L)}}$ 54

LIST OF ABBREVIATIONS

UTeM	-	Universiti Teknikal Malaysia Melaka
FKP	-	Fakulti Kejuruteraan Pembuatan
FKM	-	Fakulti Kejuruteraan Mekanikal
EDC	-	Electrical discharge coating
PMEDM	-	Powder mixed electrical discharge machining
SEM	-	Scanning Electron Microscopy
XRD	-	X-Ray Diffraction
PSA	-	Particle Size Analyzer
EDM	-	Electrical Discharge Machining
EDX	-	Energy Dispersive X-R
PVD	-	Physical Vapor Deposition
CVD	-	Chemical Vapor Deposition
RTM	-	Resin transfer moulding
SEM	-	Scanning electron microscope
PM	-	Powder metallurgical
TiC	-	Titanium carbide
Al_2O_3	-	Aluminium oxide
NbC	-	Niobium carbide
Si	-	Silicon
OHNS	-	Oil Hardening Non-Shrinkable
HC-HCr	-	High Carbon High Chromium
Al	-	Aluminium
Cu	-	Copper
Cr	-	Chromium
Mo	-	Molybdenum
SR	-	Surface roughness
MRR	-	Material removal rate
TWR	-	Tool wear rate
YZP	-	Yttria-Stabilised Zirconia Polycrystal

PVC	-	Polyvinyl Chloride
TaC	-	Tantalum carbide
W	-	Tungsten
Fe	-	Iron
hBN	-	Hexagonal boron nitride
W-Cu	-	Tungsten and copper
Mg	-	Magnesium
R&D	-	Research and development

LIST OF SYMBOLS

cm	-	Centimetre
m	-	Metre
%	-	Percent
g/cm^3	-	Grams per centimetre cube
wt. %	-	Weight percent
mm	-	Millimetre
MPa	-	Mega Pascal
GPa	-	Giga Pascal
°C	-	Degree Celsius
nm	-	Nanometre
kg.cm3	-	Kilogram centimetre cube
phr	-	Part per hundred resin
kg	-	Kilograms
mm/min.	-	Millimetre per minute
rpm	-	Revolution per minute
Ip	-	Peak current
T_{ON}	-	Pulse on time
T_{OFF}	-	Pulse off time
V	-	Voltage
HV	-	Vickers hardness
A	-	Ampere
µs	-	Micro second
g/L	-	Gram per litre
µm	-	Micro meter
cm^3/L	-	centimetre cube per litre
BHN	-	Brinell hardness number
nA/cm^2	-	Nanoampere per square centimeter
$\Omega\,cm^2$	-	Ohm per centimetre square
mm/year	-	Millimetre per year

mg/min	-	Milligram per minutes
kgf	-	Kilogram-force
ksi	-	Kilo pounds per square inch
psi	-	pounds per square inch
L	-	Litre
HK	-	Knoop hardness
HRC	-	Rockwell hardness
Mpa√m	-	Mpa per square metre
G/Cm^3	-	Grams per cubic centimetre
W/ Mk	-	Watts per metre kelvin
J/Kgk	-	Joule per kilogram per kelvin
Ω Cm	-	Ohm centimeter
Kgf/mm^2	-	kilogram force per square millimeter

CHAPTER 1

INTRODUCTION

1.1   Research Background

Surface modification or also known as surface treatment is not a new process in industry. It is widely used not only in engineering field, but also biomedical, automotive and aerospace (Mussada & Patowari, 2015). The main function of surface modification is to change and enhance the chemical, mechanical and physical properties of the material. According to Oshida (2013), by going through the surface modification process, the material not only can improve the wear resistance, but also resistance again degradation, biocompatibility, and surface wettability, this statement also supported by Shibe & Chawla (2014). In this modernization era, there are a few different technique that can be used in surface modification, which are Electrical Discharge Machining (EDM), thermal spraying, Physical Vapor Deposition (PVD), Chemical Vapor Deposition (CVD), Electroplating, Laser coating, Electron-Beam Irradiation and Sputtering (Richhariya, 2013).

EDM is a non- conventional process which is used extensively in industry for machining various conductive material with geometrically shape including difficult-to-cut material (Nanimina et al., 2014). Erosive effect of EDM firstly invented by English scientist, Joseph Priestly in 1770. In EDM, electrical energy is transformed into thermal energy and the energy is used for machining purposes (Khan & Hameedullah, 2011). A series of distinct electrical discharge are produced between the electrode and the workpiece. Electrical discharge sparking between the tool electrode and workpiece and cause the material on the substrate removed (Watane, 2017).

Surface modification of workpiece by material transfer during EDM process is known as Electrical Discharge Coating (EDC) process which is also known as a reversed

method of EDM. Watane (2017) mentioned that EDC is one of the evolving coating process due to its comfort, usability, simplicity, reliability and cost effectiveness. Surface coating is used to enhance the properties of the material, not only increasing the strength but also increase the corrosion resistance and wear resistance. EDC is a recent technology where the polarity is reversed, whereas the electrode is connected to anode and workpiece is connected to cathode (Khan & Hameedullah, 2011). In EDC, there are many ways to perform surface modification such as EDC with powder metallurgical electrodes, EDC with multi-layer electrode, EDC with powder suspension or powder mixed electrical discharge machining (PMEDM) and dry EDC (Liew et al., 2020).

In this study, we focus on the PMEDM. The performance of EDM is improved by mixing the powder into the tank that contain dielectric fluid (Nanimina et al., 2014). This process is carry on by mixing electrically conductive powder into the dielectric fluid. An energized powder particles moving and behave in zig-zag movement, then the particle will organize in chain shape and assist the bridging effect that increase the gap voltage and insulating strength of dielectric fluid (Talla, 2016).

In previous research, there are many type of powders have been used such as aluminium, graphite, silicon (Talla, 2016), chromium, copper (Fong & Chen, 2005) and etc. However, the usage of tungsten powder is rarely used in surface modification of aluminium. Therefore, the objective of this study is to investigate the effect of different peak current (I_p), pulse on time (T_{ON}) and discharge voltage (V) of tungsten powder on the characteristic of coated surface including the thickness of deposited layer and elemental composition after the EDC process.

1.2   Problem Statement

In industry especially automotive, aerospace and engineering field, aluminium is used widely due to the properties of the material. According to Karthi et al. (2018) aluminium is a kind of material that have a good conductivity, resistance to corrosion, have high thermal conductivity and light weight. Among the common metal, aluminium is the lightest metal which is three time less than steel metal (Vargel, 2004).

According to Kalpakjian et al. (2018) in fabrication of mold and die, aluminium 6000 series was commonly used. However, after some duration of time, the existence of wear and corrosion on the surface of workpiece will create defect and reduce its service life. The exposure to loads, pressure and extreme temperature during the operation of mold and die, became the main cause to the corrosion of metal (Akpan & Offiong, 2013). Therefore, deposition of material or coating is needed to cover the surface of mold an die in order to prevent it from corrode and wear which can lead to serious damage (Liew et al., 2018). Modification of aluminium surface not only can increase the hardness and thickness of coating layer of the material, but also can increase the life span which is a good investment for manufacturer to save cost (Iqbal et al., 2010).

In this study, surface modification of aluminium was carried out by using W powder suspension. EDC process was used and the peak current (I_p) and pulse on time (T_{ON}) of EDM machine were varied. The thickness of coating layer on the coated surface were investigated after the experiment.

1.3   Objectives

The objectives of this experiment are:

(a)   To characterize the tungsten powder by using Scanning Electron Microscopy (SEM).

(b)   To investigate the effect of peak current (Ip) and pulse on time (TON) on the coating layer thickness after EDC process.

1.4   Scope of Research

In this research, Sodick AQ35L die sinker machine was used to run the EDC experiment. The equipment and materials were prepared for this research including tungsten powder, aluminium workpiece, copper electrode, surfactant and kerosene oil. The parameter counted in this research is a peak current (Ip) and pulse on time (T_{ON}) that is varies while the other parameters such as voltage (V), concentration of tungsten powder and pulse off time (T_{OFF}) were constant. After the experiment, thickness of deposited layer of the modified surface was investigated.

1.5   Thesis Organization

The organization of this thesis is as following. In chapter 1, Introduction, the background of research, objectives, problem statement and the scope of research were explained. Chapter 2, literature review discussed about the theory and related previous research such as working principle of EDM, EDC, aluminium, PMEDM, tungsten powder and parameter counted in EDC. In Chapter 3, all information that relies on the methodology was explained such as the preparation of equipment and material, and experimental procedure of EDC process. Chapter 4 is result and discussion. The data and result were

discussed and extracted. Lastly is Chapter 5, conclusion and recommendation. In this chapter, all the result and data were summarized.

CHAPTER 2
LITERATURE REVIEW

In this chapter, theory and research that have been done before by various researcher will be described. Related information about EDC will be discussed and extracted to support each information.
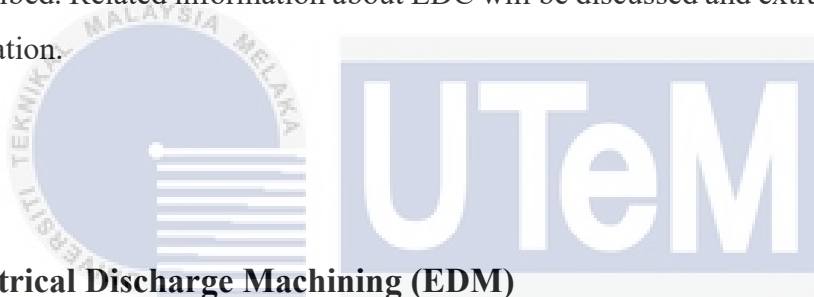
2.1   Electrical Discharge Machining (EDM)

Electrical discharge machining (EDM) is essentially a non-conventional machining process for removing material and widely used in aerospace, automotive industry and production of surgical components (Ho & Newman, 2003). This technique is widely used to cut hard material that having complex shape (Nanimina et al., 2014). In 1770, English Scientist, Joseph Priestly firstly invented the erosive effect of electrical discharge machining, however in 1943 at the Moscow University, Lazarenko used the disruptive effects of electrical discharges for structural application (Banu & Ali, 2016). B.R. and N.I. Lazarenko together conducted a research on how to minimize wear on electric power contact. Discharge of energy that generated by capacitor is tested on different materials.

2.1.1 Working Principle of Electrical Discharge Machining (EDM)

EDM is a process where electrical energy is converted into thermal energy to remove the material from the work piece (Banu & Ali, 2016). In this process, there is no physical contact between tool electrode and workpiece. Both tool electrode and workpiece are immersed into the dielectric fluid, where both of it are electrical conductor (Banker et al., 2013). DC power supply is directly connected with workpiece and electrode where the workpiece is attached to a positive terminal and the electrode attached to negative terminal. The tool electrodes travels towards the workpiece and minimize the spark gap between both tool and workpiece so that the voltage applied sufficiently strong to ionize the dielectric fluid (Bojorquez et al., 2002). A sequence of electrical discharge and high current density is occurred between the workpiece and electrode which create an electrical spark (Fong & Chen, 2005). Electric spark acts as a cutting tool to cut and erode the workpiece into the desired shape (Krar, 2016). The generation of spark between the substrate and electrode which cause the erosion of metal is known as thermoelectric phenomenon (Surekha et al., 2018). According to Mahendran et al. (2010) and Sanjeev Sharma et al.(2015), the thermal energy creates a plasma channel between the tool electrode and workpiece at a temperature between 8000°C to 12000°C. At a very high temperature, the electrode material is melted and vaporized then deposited on the surface of workpiece. Figure 2.1 illustrates the basic working Principle of EDM while Figure 2.2 illustrates the view of discharge gap.
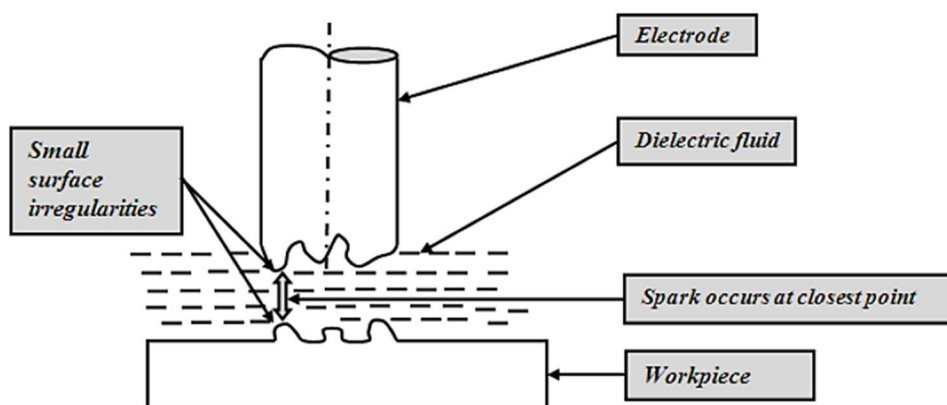
Figure 2.1: Basic working principle of EDM (McDonnell, 2010).
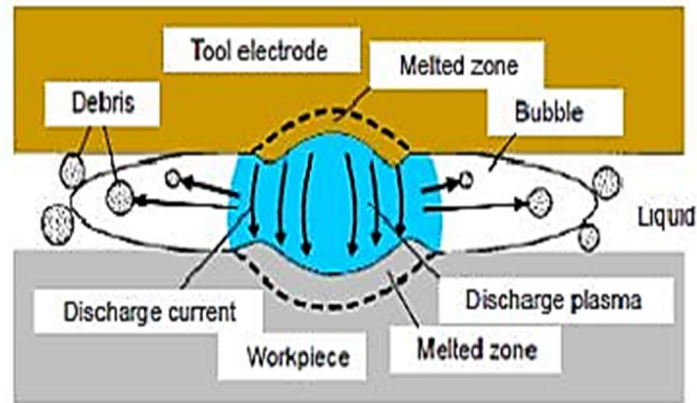
Figure 2.2: Illustrative view of discharge gap (Kunieda et al., 2005).

2.2 Electrical Discharge Coating (EDC)

Electrical discharge coating (EDC) or also known as Electrical Discharge Alloying (EDA) is a reverse method of electrical discharge machining (EDM) where the electrode polarity is converted (Chakraborty et al., 2018). There are four types of EDC that used for surface modification which include EDC with powder metallurgical electrode (PM), EDC with multilayer electrode, EDC with powder suspension or PMEDM and dry EDC (Liew et al., 2020). EDC surface alteration approach has the characteristics of high performance and low expense (Li et al., 2011). According to Ueno et al. (2016), the advantage of using EDC as a coating method is, the thickness of the film deposited on the surface of workpiece is easy to control. The hardness of the surface of the workpiece can be improved by using EDC as well as resistance to wear and against degradation (Amorim et al., 2017).

In EDM process, the removal of material from the workpiece is take places, while in EDC the electrode material is deposited on the surface of workpiece with the presence of high current electric pulse and dielectric fluid (Murray et al., 2017). The extracted tool material is collected on the workpiece surface and creates a strong coating film on the surface of the workpiece (Sahu & Mahapatra, 2018). In this process, both electrode and workpiece immersed into the dielectric fluid where the tool electrode attached to the positive terminal

8

and workpiece attached to negative terminal. The illustration of deposition of material in EDC process can be seen in Figure 2.3.
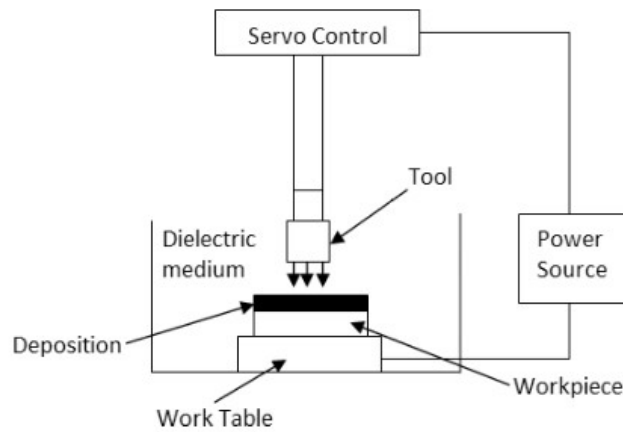
Figure 2.3: Illustration of deposition of material in EDC (Chakraborty et al., 2018).

EDC has been used in many field for surface modification recently. In this process, the material from tool electrode or powder particle suspended in dielectric fluid is transferred on the surface of the workpiece (Bui et al., 2019). According to Kumari (2015) the deposition of material on the workpiece surface after the EDC process will enhance the surface properties such as surface hardness, wear resistance, oxidation and corrosion resistance.

In Algodi et al. (2016) research, electrical discharge coating technique is used to modify the surface of 304 stainless steel by using PM titanium carbide (TiC) tool electrode. The result shows that, there is an improvement in mechanical performance of the workpiece where the surface hardness is increase after go through EDC surface modification. This condition is depends on several machining condition such as current, pulse on time and the content of the deposited material (Algodi et al., 2015).

According to Janmanee & Muttamara (2012), in their research on surface modification of tungsten carbide by using EDC technique, the micro cracks that occur on EDMed surfaces is reduced and the surface hardness of the workpiece is improved due to

the presence of titanium powder in the machining gap where the titanium powder filled the micro crack.

Khan et al. (2012) reported that, when the current is increased, thicker recast layer is observed occur on the mild steel workpiece surface when a powder particle of titanium carbide (TiC) and aluminium oxide (Al_2O_3) is added into the dielectric fluid in EDC process. In orthopaedic application, the usage of PMEDM method show that there is an improvement of wear resistance and tribological performance of β-Ti implant. The result shows that, TiC, niobium carbide (NbC) and silicon carbide (SiC) material is deposited in the surface of the workpiece (Prakash et al., 2015).

In Sumi et al. (2012) research, TiC electrode containing Silicon (Si) is used to machine the surface of austenitic stainless steel SUS304 workpiece by using EDC technique. They found that the surface roughness of the workpiece and the defect that occur on the surface of the workpiece is decreased when more Si is contained in the electrode. After machining process, the properties of surface workpiece may change when the materials from tool electrode or addition of powder in dielectric transferred on the surface (Kumar et al., 2009).

2.2.1 Working Principle of Electrical Discharge Coating (EDC)

Working principle of Electrical Discharge Coating (EDC) is similar with the Electrical Discharge Machining (EDM) process. Generally, in order to get the desired coating layer on the surface of the workpiece, the tool electrode and dielectric fluid are modified. In EDC process, the polarity is reversed. Tool electrode is attached at positive terminal and workpiece is attached at negative terminal of power supply (Tyagi et al., 2018). During the generation of electric spark, melting and vaporization process of workpiece material takes place in micro plasma channel due to the high temperature and cause the material from the electrode melted and deposited on the surface of the workpiece. Due to the low temperature of dielectric fluid, the material of the workpiece gets solidified during each

electric spark by a rapid cooling process (Kumari, 2015). Figure 2.4 shows the schematic view of EDC working principle.
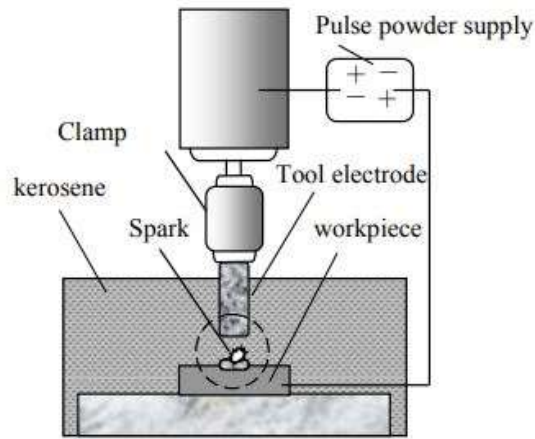
Figure 2.4: Schematic view of EDC (Kumari, 2015).

2.3   EDC with Powder Suspension or PMEDM

PMEDM or also known as Additive Mixed EDM (AMEDM) or EDC with powder suspension is a process where the powder particle is added in the dielectric fluid (Garg et al., 2010). According to Murray & Clare (2016), EDC can produce a coating layer on workpiece surface where the coating material come from tool electrode or powder suspension in dielectric fluid. Both method can provide a thick and thin layer on the surface. Whenever the spark is generated between the tool electrode and workpiece surface, the powder material will deposited on the workpiece (Mussada & Patowari, 2015). PMEDM commonly used in automotive and aerospace industry to modified the surface of light metallic alloy in order to improve the wear resistance (Talla, 2016).

In Janmanee & Muttamara (2012) research, titanium powder is added into the dielectric fluid in EDC process to modified the surface of tungsten carbide. After the EDC

process, it is observed that the surface hardness is increase and less crack occur on the surface of tungsten carbide where the micro hardness that obtained is between 990 HV to 2750 HV.

From the experiment conducted by Kumar & Batra (2012), tungsten powder is used as an additive material in dielectric fluid to modify the surface of this three types of die steel material which is Oil Hardening Non-Shrinkable (OHNS) die steel, High Carbon High Chromium (HC-HCr) die steel and Hot work type H13 die steel. The parameter counted is peak current (2, 4, 6 A), pulse on time (5, 10, 20µs) and pulse off time (38, 57, 85µs). From the micro hardness test that have been conducted after the surface modification process, it was observed that there is a potential the amount of tungsten can reach 3.25% in the machined surface of H13 die steel by using EDC technique.

Panda (2019) study the effect of PMEDM on surface hardness of AISI D3 Die Steel. The dielectric fluid mixed with different concentration of manganese powder (5, 10 & 15 g/L) while the electrode used is copper and graphite. Reverse polarity is used in the experiment. The result shows, the micro hardness of the workpiece hit 2815 HV when the manganese powder is added into the dielectric fluid and using graphite electrode compared to un-machined workpiece which contain 710 HV and 1242 HV. This proved that, the usage of manganese as a powder addition in EDC process can improve the hardness of die steel. This kind of method can be applied on dies and press tools in order to keep it long lasting.

Tijo & Masanta (2017) stated that the decomposed carbon that contain in the dielectric fluid will react with the powder particle that added into the fluid. This reaction produces metallic carbide, a hard layer coating that deposited on the surface of the workpiece. In their research, they revealed that the addition of powder in EDC process on the surface morphology of the coating is affected by peak current and duty factor. In the other hand, the result also showed that the micro hardness on the workpiece surface is increasing by three time.

2.3.1 Working Principle of PMEDM

In PMEDM, the powder is mixed together with the dielectric fluid. Negative polarity is used where the electrode placed at positive terminal, while the workpiece placed at negative terminal in order to allow the coating process instead of removal process. The formation of plasma channel in between the surface of tool electrode and workpiece will melt the powder particle that suspended in the dielectric fluid when the electrical discharge is generated. A very high temperature of electrical sparking causes the melting and evaporation process in plasma channel. This phenomenon causes the melted powder to deposited on the surface of the workpiece. The powder that deposited on the workpiece then will be solidified by rapid cooling process or quenching every time when the electrical discharge sparking. This process make a deposited powder bond together with the workpiece surface to form a coating layer (Liew et al., 2020). Figure 2.5 shows the illustration of PMEDM experimental setup in EDC process. Talla (2016) reported that the surface finish of the workpiece and the machining rate is better compared to conventional EDM if suitable powder particle is added into the dielectric fluid. Based on the previous research that has been done by previous researcher, Table 2.1 shows the summary of the effect of different size of powder particle in PMEDM process.

1 - Magnets   2 - Circulation Pump   3 – Work tank   4 - Nozzle
5 - Machining tank 6 - Workpiece   7 - Electrode   8 - Stirrer
9 - Oscilloscope   10 - Recorder   11 - ZNC generator   12 - Power supply
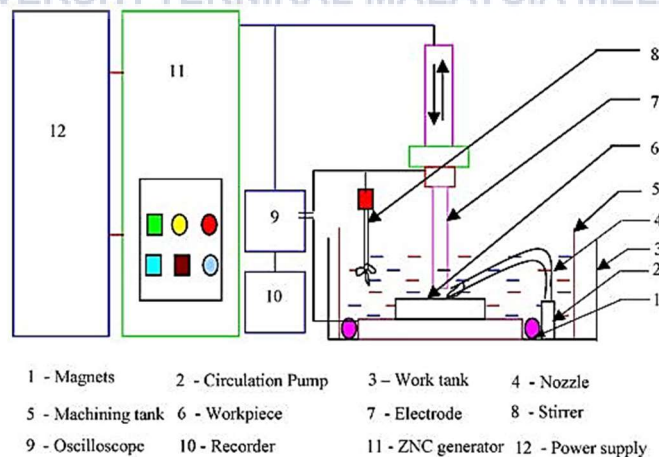
Figure 2.5: Illustration of PMEDM experimental setup (Kansal et al., 2007).

Table 2.1: Summary of previous research on effect size particle of powder in PMEDM.

No.	Author	Types of particles	Particle size	Results
1	Amorim et al. (2017)	Molybdenum (Mo)	1) 5 µm 2) 15 µm	5 µm: The deposition layer does not cover the surface completely and crack is occurred. 15 µm: Layer deposited on the workpiece surface completely and uniformly.
2	Tzeng & Lee (2001)	Aluminum (Al), chromium (Cr), copper (Cu) and silicon carbide (SiC)	1) 0.07-0.08 µm 2) 10-15 µm 3) 100 µm	Material removal rate (MRR): MRR increased as the size of particle is increased. Tool wear rate (TWR): TWR decreased when the size of particle increased.
3	Fong & Chen (2005)	Aluminum (Al), chromium (Cr), copper (Cu) and silicon carbide (SiC)	1) 0.07-0.08 µm 2) 10-15 µm 1) 100 µm	Surface roughness (SR): 0.07-0.08 µm produced the best surface finish while 100 µm produced the worst surface finish. Recast layer: 0.07-0.08 µm generates thicker recast layer while 100 µm powder size generate thinnest recast layer.
4	Jabbaripour et al. (2013)	Aluminum (Al)	1) 2 µm 2) 20 µm 3) 63 µm	Material removal rate (MRR): MRR decreased when the Al powder particle size is increase. Surface roughness (SR): SR is better when the size of Al powder is increased.

14

As can be seen in Table 2.1, it is proved that the size of particle effect the SR, MRR, thickness of recast layer and TWR of the workpiece material in EDC process.

2.4   Tungsten (W)

In 1779, an English Chemist Peter Woulfe is the first person who discovered a gray-white metal that is known as a wolframite. While in 1783, Juan Jose and Fausto Elhuyar success to isolated the wolframite that consist of tungsten (W) by heating it using carbon which reduce the wolframite acid and turns it into W. Commonly W found in the mineral of scheelite and wolframite that is harvested form earth crust and commonly hydrogen or carbon will be used to reduce the tungsten oxide (Gregersen, 2020).

According to EPA (2014), W is part of the refractory metal group that has a very high melting point among other common metal with very low pressure of vapour. W known as a high electrical conductivity metal where it also can resist corrosion, while for chemical reaction, it acts as catalyst. However, due to the application and demand in industry, W powder commonly added with other element to improve the mechanical and chemical properties. Due to its unique characteristic, it is widely used in aerospace, military, automotive and nuclear industry (Zhu et al., 2017).

Table 2.2: Properties of tungsten powder (Matmatch, 2020).

Properties of material	Value
Melting point	3420°C
Boiling point	5555°C
Density (RTP)	19.3 g/cm^3
Thermal conductivity	173 W/(m.K)
Hardness (Mohs)	7.5
Young's modulus	405 Gpa
Tensile strength	980 Mpa
Atomic number	74
Atomic weight	183.84

Kanpara et al. (2014) use W powder as an additive in atmospheric plasma spraying to coat the SS304 steel surface. As a result, the formation of thick coating layer with the thickness for about 200 μm was observed deposited uniformly on the workpiece. Ultrasonic C-scan also conducted to investigate the bonding between the W and workpiece. From the result obtained, both W and workpiece shows a good bonding which improve the hardness of workpiece.

On the other hand, Liew et al. (2018) reported that, when W powder was added into the dielectric fluid during the EDC process, the micro-hardness of the aluminium workpiece shows an increment for about 104.86%. The micro-hardness of the substrate before the coating is 106.67 HV, however after the EDC process, the micro-hardness value is at 218.33 HV. The increment of the micro-hardness is due to the deposition of W powder that melted during the machining process.

Dong & Lu (2017) investigate the mechanical properties of AlCoCrFeNi2 alloy by adding W in the process of arc melting. As a result, the addition of W improve the mechanical properties of workpiece such as strength of yield and the hardness. From the result obtained, the hardnes was increased from 293 HV to 356.2 HV and the yield strength was increase from 575.5 Mpa to 651.5 Mpa, while the fracture strength was observed at 2785.9 MPa. The increment of hardness was due to the presence of W powder that dissolve well in the FCC and BCC phase which create an increment in volume fraction.

In medical application, Radu et al. (2019) discovered that, the addition of tungsten into Ti-15Mo-W alloys that used for artificial implant devices improve the mechanical properties and elasticity of the alloy. According to Niinomi et al. (2016), to produce good artificial implant, there is a few characteristic need to be counted such as resistance to wear and corrosion, have an elastic modulus between the range of 17-30 Gpa which is close to human bone and also have an excellent strength. The result obtained from Radu et al. (2019) research shows that the microhardness of Ti-15Mo-W alloys added with tungsten increases from 248 to 327 HV. The value of compressive strength also shows an increment from 782 to 921 Mpa with no formation of crack found. While the elastic modulus of the material is

within the range of 17.86 to 23.27 which is the best range of elastic modulus as mentioned by Niinomi et al. (2016).

2.5   Parameter in PMEDM

2.5.1   Powder Concentration

According to Marashi et al. (2016), the appropriate concentration of powder can contribute to efficiency and stability of the process. Kumar & Davim, (2011) studied the application of silicon powder as an addition in PMEDM. The result showed that, the machining rate is triplicates and the surface roughness decreased by 33% by adding the appropriate amount of silicon powder which is 4 g/L to the EDM dielectric fluid. However, the powder characteristic makes the optimum concentration of each powder is different in order to maximizing the performance.

Prakash et al. (2017) revealed that the concentration of silicon significantly affect the recast layer of Ti-35Nb-7Ta-5Zr β Titanium Alloy workpiece. The result shows that, at 2 g/L concentration of silicon powder, the recast layer thickness shows a reduction from 12 μm to 8 μm. When the concentration is increased to 4g/L, the thickness of recast layer is about 3μm, however, when the concentration is increased to 8 g/L, it is clearly can be seen that the layer thickness is increased to 15-20 μm. This situation happen because high concentration of powder is trapped together with the eroded material between the discharge gaps and cannot be flush easily which cause the powder to deposit on the workpiece surface.

Fong & Chen (2005) used three level of powder concentration for aluminium (Al), chromium (Cr), copper (Cu) and silicon carbide (SiC) which is 0.25, 0.5 and 1.0 cm^3/L. As a result, it can be seen that the thickness of recast layer on the workpiece surface is increase when 0.5 cm^3/L of powder concentration is applied. However, thinnest recast layer is observed when the concentration is at 0.25 cm^3/L and 1.0 cm^3/L. Fong & Chen (2005a)

stated that, both 0.25 and 1.0 cm³/L powder concentration produced thinnest recast layer is due to their accumulated heating effect is weak compared to 0.5 cm³/L powder concentration. Figure 2.6 shows the effect of powder concentration on the thickness of recast layer.
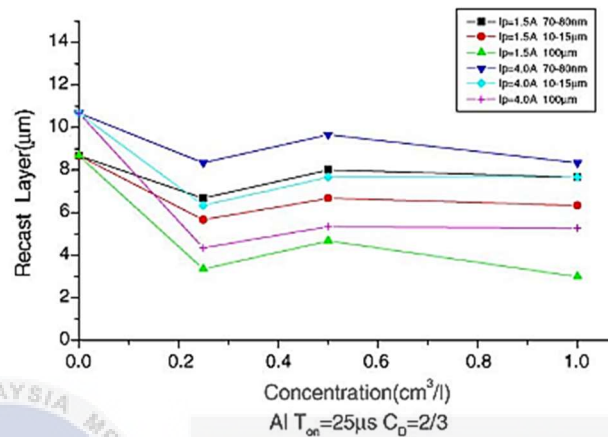
Figure 2.6: The effect of powder concentration on the thickness of recast layer(Fong & Chen, 2005).

2.5.2 Peak Current

Peak current is the amount of power used in EDM where the measurement unit is in Ampere. Peak current is essentially very significant and the most influencing factor in EDM (Garg et al., 2010). In general, peak current is described as the maximum amount of current that provides support to the output to perform a certain task. In EDA or EDC operation, the peak current is described as the maximum input current that generates spark between the electrode and workpiece submerged in dielectric fluid (Liew et al., 2020). The current rises during each on-time pulse, until it hits a pre-set level that is represented as the peak current (Mahendran et al., 2010). Higher amperages is used in roughing operations or cavities in large surface areas. Machining performance often relies on peak current, the usage of higher current definitely will improve the MRR, however it will give some effect towards surface finish and tool wear (Singh & Bhardwaj, 2011).

Mussada & Patowari (2015) stated that the peak current has a significant impact on the thickness of the coating layer. A recent study carried out by Tyagi et al. (2020) showed that minimum layer thickness of 0.446 mm was achieved when a low peak current of 4 A was applied and a maximum layer thickness of 0.647 mm can be obtained at a strong peak current of 10 A. This occurrence was attributed to the high peak current produced intense spark and allowed more content to melt and eventually settle on the surface of mild steel.

Singh & Bhardwaj (2011) stated that the usage of high peak current that exceed the need to remove the material will cause the thermal damage to the tool electrode because of the spark temperature is high. However, by decreasing the peak current and increasing the spark duration will help in lowering the tool wear and increase the efficiency of the machining.

Janmanee & Muttamara (2012) stated that, the titanium coating layer deposition on the surface of tungsten carbide is influenced by the current value. The value of current is varying by 10, 15, 20, 25 (A). It is observed that 20 A is the optimum value of current for combining titanium powder with the surface of the workpiece during recasting. However the bonding potential reduces until the current reaches 20 A. Figure 2.7 shows the variation of current applied that effect the percentage weight of Ti coating.
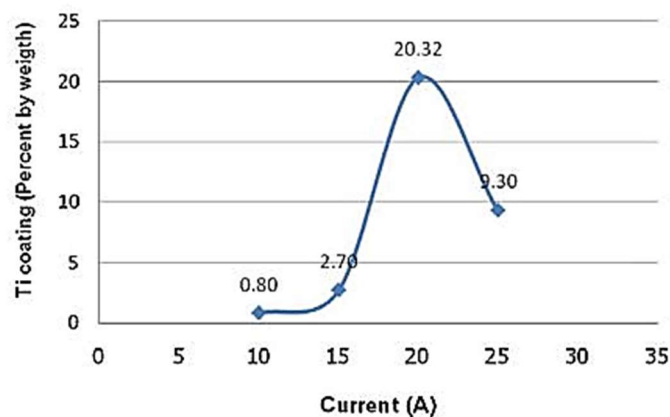
Figure 2.7: Variation of current applied that effect the percentage weight of Ti coating
(Janmanee & Muttamara, 2012).

A recent research by Liew et al. (2018) revealed that the increment of peak current effect the weight percentage of deposited layer. They reported that, when the peak current is increased from 3A to 5A, the average of weight percentage of deposited tungsten also increased. This situation happens because peak current enables the substance trapped in the dielectric fluid to be quickly moved to the surface of the component. Increases in peak current could lead to large amounts of melted material and promote deposition and decomposition of powder during EDC. However, different situation is happen with carbon deposited layer. The weight percentage of carbon is decreased along with the increment of peak current. This may be attributed to the phenomenon of sparking on the workpiece surface, which grew greater as peak current rose and more fused material was expelled from the workpiece surface. Figure 2.8 shows the effect of weight percentage of deposited tungsten and carbon that influenced by the peak current value.
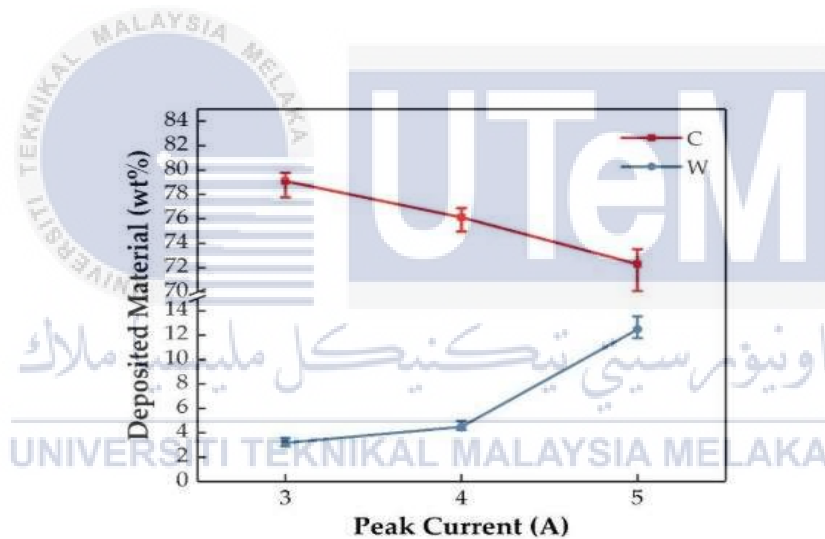
Figure 2.8: The effect of weight percentage of deposited tungsten and carbon that influenced by the peak current value (Liew et al., 2018).

2.5.3   Pulse On Time

Pulse on time is a length of time that allow current to flow per cycle (Ramabalan, 2015). The measurement units of pulse on time and pulse off time is microseconds (Mahendran et al., 2010). During pulse on time, the electrical discharge operation is performed. The gap between the electrode spark is bridged, the current is produced between

the surface of the work-piece and the electrode of the device and the task is done (Richhariya, 2013). The duration of pulses and the number of cycle per seconds are important since all the work is produced during the pulse on time (Mahendran et al., 2010). Figure 2.9 shows the illustration of electrical discharge condition.
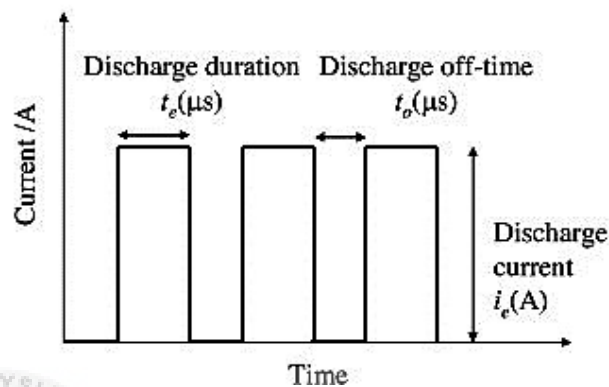
Figure 2.9: Illustration of electrical discharge condition (Ueno et al., 2016).

According to Chakraborty et al. (2018), large amount of workpiece will be melted if the pulse duration is longer. Longer pulse duration provides a broader and deeper hole compared to shorter pulse duration. Since the hole has a rough surface coating, the longer pulse length would allow further heat sink into the workpiece and therefore it will expand, resulting in a wider recast layer and a deeper heat region (Mahendran et al., 2010). Rahang & Patowari (2016) also stated the amount of tool wear can be controlled by pulse on time where the duration of time can be set at each pulsed of energy discharged.

Liew et al. (2018) reported that, there is a relationship between the pulse on time and weight percentage of deposited layer of tungsten and carbon. In their result, it is showed that the average weight percentage of tungsten and carbon is decreased when the value of pulse on time is increased from 150 µs to 250 µs. According to Ekmekci et al. (2015), this situation happen because as pulse on time decreases, the size of the plasma channel extends and the distance travelled by the particle suspension to the workpiece surface rises.

Tijo & Masanta (2014) revealed that, the most significant factors affecting the rate of deposition are pulse on time. In their study, green compact electrode with the mixture of tungsten and copper powder is used. It is observed that, the optimum parameter for higher deposition rate is at 200 µs pulse on time with 150 Mpa compaction pressure and 3A peak current. However, when the pulse on time reached 300 µs, it is clearly showed that the deposition rate is decreased. This condition occurs because the rough and porous coating was generated at high pulse on time and the coated substance was improperly bound to the workpiece which result to decreasing in weight percentage of deposited layer.

Ueno et al. (2016) stated that, the thickness of deposited layer is increased along with the discharge duration or pulse on time. In Figure 2.10, the cross sectional SEM images of the machined surfaces shows the difference on the thickness of deposited layer when the pulse on time that applied is 8 µs and 100 µs with different machining time. It is observed that, the thickness of deposited layer is thicker when the pulse on time is at 100 µs compared to the thickness of deposited layer when the pulse on time is at 8 µs. Figure 2.11 shows the relation between deposited layer thickness and condition of the electrical discharge.
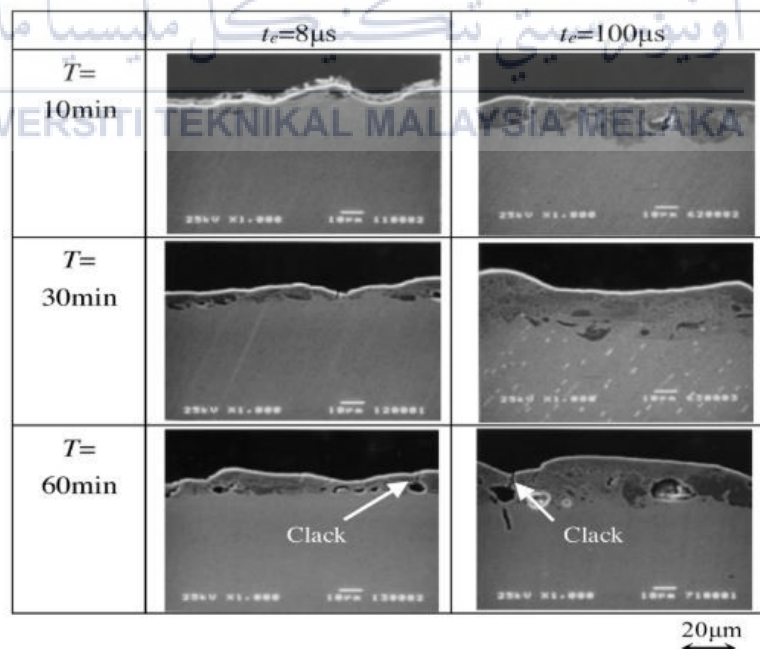
Figure 2.10 Cross sectional SEM images of the machined surfaces shows the difference on the thickness of deposited layer(Ueno et al., 2016).

22
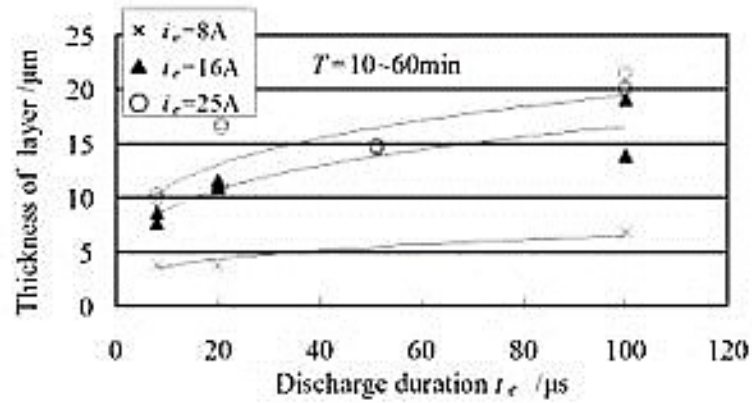
Figure 2.11: Relationship between deposited layer thickness and condition of the electrical discharge (Ueno et al., 2016).

Furutania et al. (2001) found that a smooth surface and a thick deposited layer are observed when negative polarity is applied on the electrode. Beneath low discharge current and a short pulse duration, thick accretion is achieved. In the case of negatively polarized electrode, the thickest layer is obtained with 3 A as a peak current and 2 µs as a pulse duration.

2.5.4 Pulse Off Time

Pulse off time or also known as pulse interval. It is a duration of time between each spark. Re-ionization of dielectric takes places during pulse off time and result to the efficiency of process (Chakraborty et al., 2018). In this situation, the pulse off time also regulates the process stability or leads to erratic behavior of the servo control process, while the process efficiency increase due to the drops of inter-electrode gap temperature (Richhariya, 2013). Each pulse create spark when they are in ideal condition. However, in Kumar et al. (2009) researh, the improper setting of duration and interval will make many pulse fail. This condition make the machining accuracy loss and its called as open pulse.

According to Fuller (1996), during the pulse off time, the machining speed and stability of cut will be effected. Faster machining operation occurred when the interval

23

duration shortens. However, the debris of eroded workpiece material will not be flushed away along with the dielectric fluid and the deionization of dielectric fluid will not happen when the interval is too short, where it will result to instability of the next spark. Prolonged machining time happened due to unstable spark that cause erratic cycling. In order to prevent sparking continued at one point, pulse interval must be greater than the deionization time.

Zain et al. (2014) found that the value of pulse off time gives effect towards surfaces micro hardness. Addition of tantalum carbide (TaC) into the dielectric fluid influence the surface hardness with variable parameter. The result of the investigation show that the micro hardness of the coating on the stainless steel workpieces shows an increment from 600 HV to 800 HV when the pulse off time increased from 5µs to 8µs.

Algodi et al. (2018) reported that during the pulse off time with the value 10 µs, it is observed that the temperature of the stainless steel workpiece surface that coated with titanium carbide (TiC) is rapidly reduced from 20 000 K to 4 000 K followed by a low uniform cooling rate with the valaue of 10 µs. Heat transfer between the molten fluid and the circulate dielectric fluid cause the rapid cooling on the workpiece surface. From the sitution, it is clear that the increment of pulse off time value increase the micro hardness of the workpiece.

In Kumar & Batra (2012) research, it is observed that pulse off time give more contribution to the enhancement of micro hardness of the coated workpiece (compared to pulse on time. This ensures that the pulse off-time is important and adequate idle time is necessary for the work surface to cool down and recover the sparking production. Figure 2.12 shows the percentage of contribution for micro-hardness of the workpiece.

Parameters	Work material		
	OHNS	D2	H13
Optimum setting	$A_2B_2C_3$	$A_2B_2C_3$	$A_2B_2C_3$
Peak current contribution	71.9%	73.6%	74.6%
Pulse on-time contribution	10.1%	9.2%	8.1%
Pulse off-time contribution	17.7%	16.9%	17.0%

Factor A represents peak current and level $A_1 = 2\,A$, $A_2 = 4\,A$, $A_3 = 6\,A$.
Factor B represents pulse on-time and level $B_1 = 5\,\mu s$, $B_2 = 10\,\mu s$, $B_3 = 20\,\mu s$.
Factor C represents pulse off-time and level $C_1 = 38\,\mu s$, $C_2 = 57\,\mu s$, $C_3 = 85\,\mu s$.

Figure 2.12: Percentage of contribution for micro-hardness of the workpiece (Kumar & Batra, 2012).

2.5.5 Discharge Voltage

Discharge voltage is a voltage that generated between the workpiece and tool electrode when the circuit is supplied with DC power supply (Ramabalan, 2015). In EDM process, discharge voltage is an important parameter where it related to breakdown strength of dielectric and spark gap (Kansal et al., 2005).

An ionization channel is developed before current starts to flow with the help of dielectric fluid due to the increment of open gap voltage. The voltage will drop and stabilizes at the working gap level once the current starts flowing. The gap between the workpiece and tool electrode increase when a higher voltage applied and the condition will enhance the flushing condition and helps to maintain the cut (Kumar et al., 2009).

A recent study by Prakash et al. (2018) recognized that voltage was a major influence in the thickness of the recast layer. They reported that more heat energy was transmitted to the Ti6Al4V electrode, as voltage increased from 20 to 40 V. This phenomenon caused electrode melting and increased the diffusion into the nickel workpiece and lead to increment of the recast layer thickness.

Liew et al. (2013) reported that when a low voltage (60 V) was applied, a large quantity of tungsten particle deposited on the workpiece surface. However, when the applied voltage is increases from 60 V to 110 V, the amount of tungsten deposited on the workpiece surface decreases immediately. From the situation, it is clearly shows that when the voltage rises, the weight percentage of accumulated tungsten content decreases.

According to Chung et al. (2007), discharge energy influence the spark gap where when the voltage increase, the gap also increase. At a low voltage, there is only a small gap produces in between the workpiece and tool electrode. The tungsten debris deposited on the surface since it cannot be removed effectively due to the small gap. Therefore Liew et al. (2013) stated that the sparks gap become larger when the value of voltage increase, which effect the removal of tungsten debris become easier and cause the material deposition decrease.

2.6 Properties in PMEDM

2.6.1 Surface Hardness

According to Aydemir et al. (2011), hardness is characterized as a material resistance to different forms of permanent shift in shape and penetration by another tougher material. Generally, Rockwell, Brinell, Vickers, Knoop and instrumented indentation is used to measure the hardness of material. However Verdins et al. (2013) stated that the selection for hardness test method is depend on the surface roughness, shape aspect, dimension and the microstructure. Usually, Brinell hardness test is done for material that have a rough surface, while Vickers and Rockwell hardness test usually used for material that have smooth surface.

In Watane (2017) research, Brinell hardness test is used to identify the surface hardness of the material. In Brinell hardness test, a hardened steel ball with a specified diameter that

act as a load is applied to the surface of tested material. After the load is applied on the tested material, the permanent diameter that detected on the material surface is measured and calculated. Table 2.3 shows the result of Brinell hardness number (BHN) before and after coating process. Watane (2017) also mentioned that the composition of Ti and Cu in electrode effect the value of Brinell hardness number. As shown in Figure 2.13, the value of BHN is increased when the composition of Cu increased.

Table 2.3: The Brinell hardness number before and after coating process (Watane, 2017).

Experiment No	Hardness Before Coating (BHN)	Hardness After Coating (BHN)
1	128	164
2	132	172
3	128	168
4	134	165
5	132	190
6	136	188
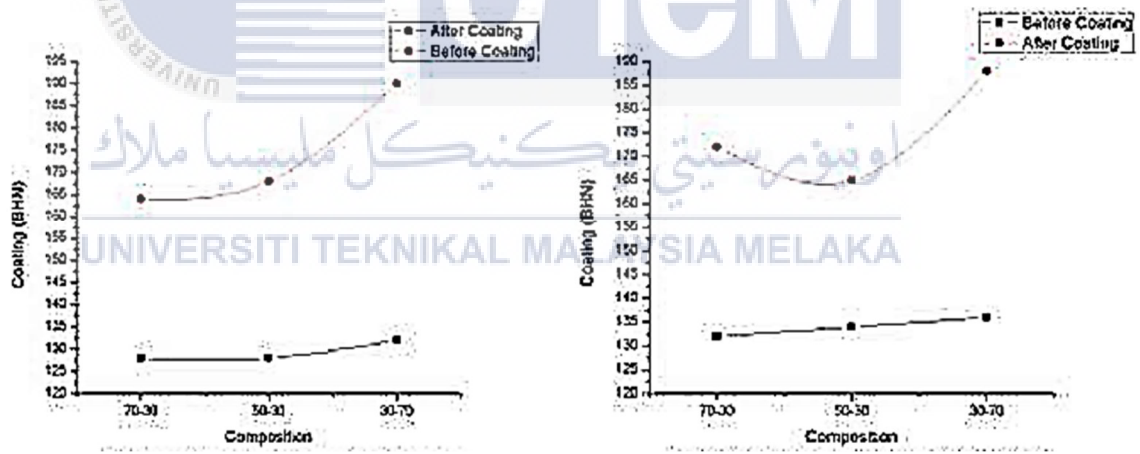
Figure 2.13: Relationship between composition of Ti and Cu and the value brinell hardness number (Watane, 2017).

Prakash & Uddin (2017) reported that the micro hardness of β-Ti implant increased due to the deposition of HA-containing bioceramic layer on it. The result that obtained by using Vickers hardness test method shows the micro hardness is increased from 390 HV to 1275 HV. The presence of HA-containing bioceramic layer on the β-Ti implant surface enable β-Ti implant to expose in corrosive condition since HA-containing bioceramic layer improved the corrosion resistance and act as a preventive layer.

27

Algodi et al. (2016) found that there is an interaction between the discharge current and the micro hardness value. The increment of current discharge lead to high weight percentage of Ti that deposited on 304 stainless steel, where the increment of weight percentage of Ti that deposited increase the value of micro hardness that tested by using Vickers hardness test. However, the increment on pulse on time vice versa with current discharge. The value of micro hardness test is decreases along with the increment of pulse on time. As a result, the optimum value for current and pulse on time to produce a good hardness level is around 2-10 A and 2-8 µs. Figure 2.14 (a) shows the relationship between discharged current with micro hardness value while Figure 2.14 (b) shows the relationship between pulse on time and micro hardness value.
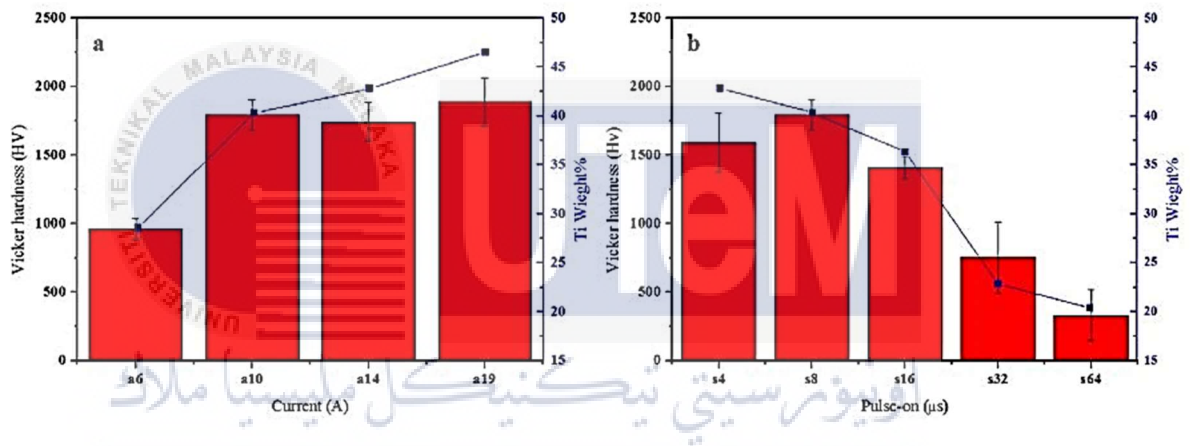
Figure 2.14: Vickers hardness test result shows the relationship between (a) current and (b) pulse on time with micro hardness value (Algodi et al., 2016).

Liew et al. (2018) recognized that the micro hardness of aluminium increased when tungsten powder is added into the dielectric fluid. After undergone the EDC process with the machining parameter of peak current (I_p) = 3 A, voltage (V) = 40 V and pulse on time (T_{on}) = 150 µs, it is observed that the micro hardness is increased from 106.67 HV to 218.33 HV which lead to 104.86% increment. The rise of micro hardness value in aluminium is due to the chemical reaction between aluminium and air which forms aluminium oxide during cooling process. Table 2.4 shows the result of micro hardness that obtained after the EDC process.

Table 2.4: The value Micro-hardness of Aluminium material before and after EDC process
(Liew et al., 2018).

Workpiece	Micro-Hardness (HV)		
	Before machining	After machining	% increase
3A, 150 µs, 40V	106.67	218.33	104.86

As reported by Janmanee & Muttamara (2012), at high temperature the re-solidification process is really fast and cause the microstructure of the machined surface layer change and the layer is known as a recast layer. Cross sectional image from Figure 2.15 shows the hardness of each level of layer. 3 level of layer is identified on tungsten carbide surface. Base material is place at the lowest layer which contain tungsten carbide WC-Co. WC+ Co + Ti placed at second layer while the generation of Ti and C is placed at the top. The top layer is a new coating surface where the generation of hard layer of Ti and C that exist on the top layer is caused by reaction of carbide in atoms diffusion process. As can be seen from the relationship between the depth of coating layer from surface (µm) with hardness of coating layer (HV), the thinner the depth of coating layer from the surface, the higher the hardness of the layer.
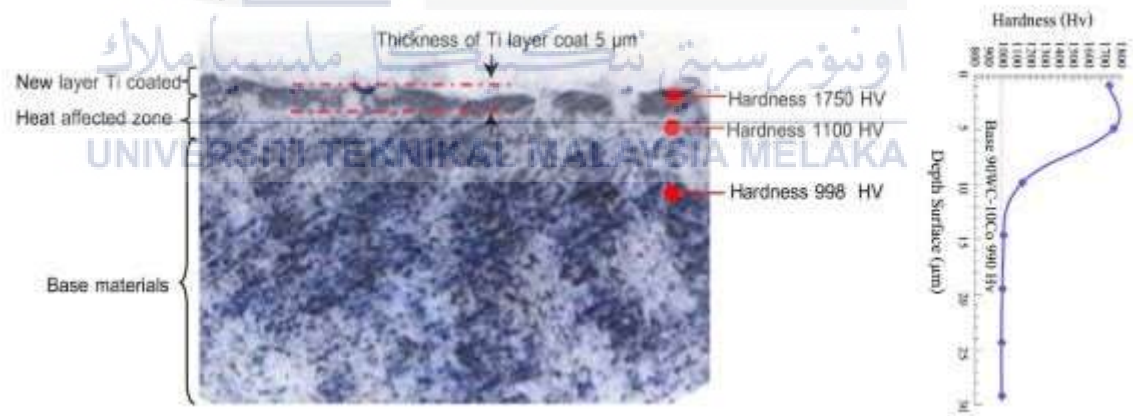
Figure 2.15: Three layer of deposited material that have different hardness (Janmanee & Muttamara, 2012).

2.6.2   Thickness of Deposited Layer

According to Prakash & Uddin (2017), after the EDC process conducted, the thickness of the deposited layer is counted by the depth of coating layer from the top of workpiece. In order to measure the thickness of the layer, cross sectional morphology is used. In their research, it is shown that the thickness of deposited layer that obtained is around 18-20 μm which contained biocompatible phase. A mechanical interlock is formed in between the base and deposited material since the metallurgical bonding is generated from the base material. Figure 2.16 shows the deposited layer of hydroaxyapatite powder on a β-phase Ti implant that varies with the powder concentration (0, 5, 10 and 15 g/L).

Figure 2.16: Image of thickness of deposited layer varies with powder concentration (0, 5, 10 and 15 g/L) (Prakash & Uddin, 2017).

Mussada & Patowari (2017) stated that EDC process is one of a process that can modify the surface of workpiece by depositing material on it. Generally, this process is performed by using EDM die sinker machine. The thickness of deposited layer can be gained by controlling and monitoring the process parameter. Figure 2.17 shows the deposition of W-Cu powder on mild steel workpiece. The same result also obtained from previous research by Patowari et al. (2015), with the usage of W-Cu P/M electrode that perform by using EDM die sinker machine,C-40 steel surface shows an improvement. From the combination of various parameter, it is observed that the thickness of layer that deposited on the workpiece is around 3-785 μm.
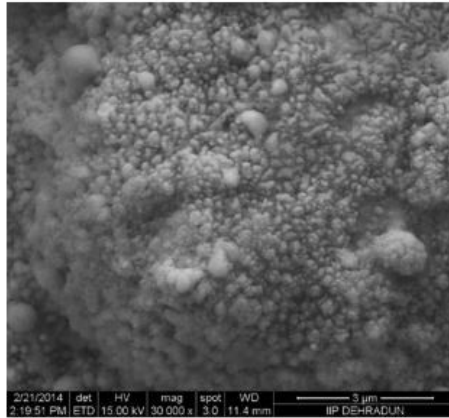
Figure 2.17: Deposition of W-Cu powder on mild steel workpiece after EDC process
(Patowari & Mussada, 2017).

Tijo & Masanta (2017) in their study revealed that, the increment of peak current (3A - 5A) caused the thickness of the coating layer increased. However, when the peak current at 6A, the thickness of coating layer reduce automatically. Figure 2.18 reveals the effect of peak current and duty factor towards thickness of coating layer. This finding has been supported by Janmanee & Muttamara (2012) who found that the current and duty factor parameter effect the composition of substance weight that deposited on the workpiece. Figure 2.19 and 2.20 reveal the effect of peak current and duty factor towards weight percentage of Ti powder.
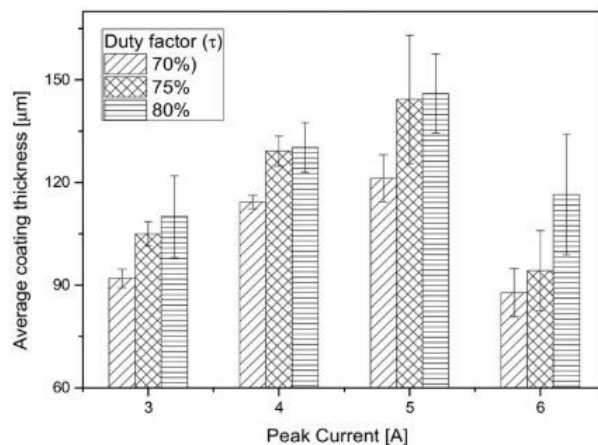
Figure 2.18: Effect of different peak current and duty factor towards thickness of coating layer (Tijo & Masanta, 2017).
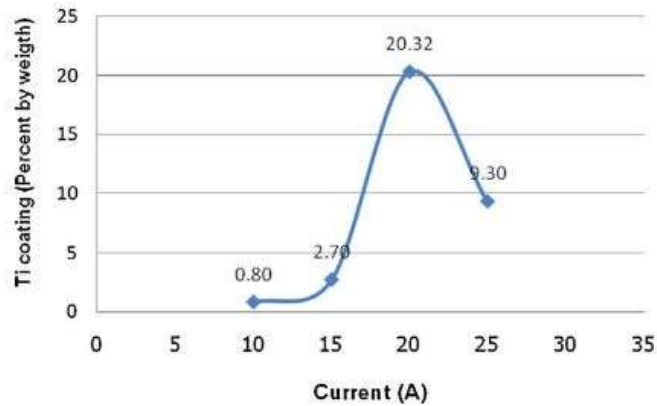
Figure 2.19: Current vs Ti coating weight percentage (Janmanee & Muttamara, 2012).
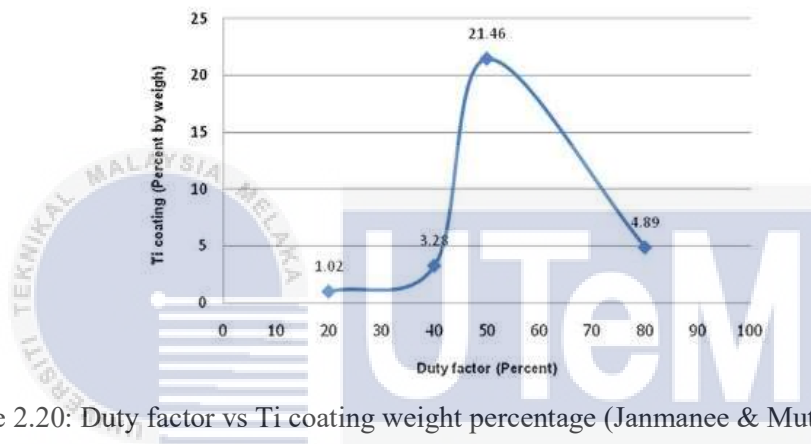
Figure 2.20: Duty factor vs Ti coating weight percentage (Janmanee & Muttamara, 2012).

Chen et al. (2014) mentioned that the increment of Ti powder concentration in dielectric fluid increase the thickness of coating layer. About 4-11 µm thickness of deposited layer was found is formed on the workpiece surface when the concentration of Ti powder is increased to 6 g/L compared to 3 g/L Ti powder concentration added into the dielectric fluid where the thickness of deposited layer that obtained is about 3-10 µm.

2.6.3 Elemental Composition

According to Mazarbhuiya et al. (2020), the existence of tool or powder material on the deposited layer can be detected by using X-Ray diffraction (XRD) analysis. The existence of the material can be observed from the peak in XRD profile. In their research, the surface of CFRP is modified by using EDC method where tungsten-copper is used as

tool electrode. From Figure 2.21, it shows that tungsten and copper that produced from erosion of tool electrode is transferred on the surface of workpiece with different discharge current (6A and 8A).
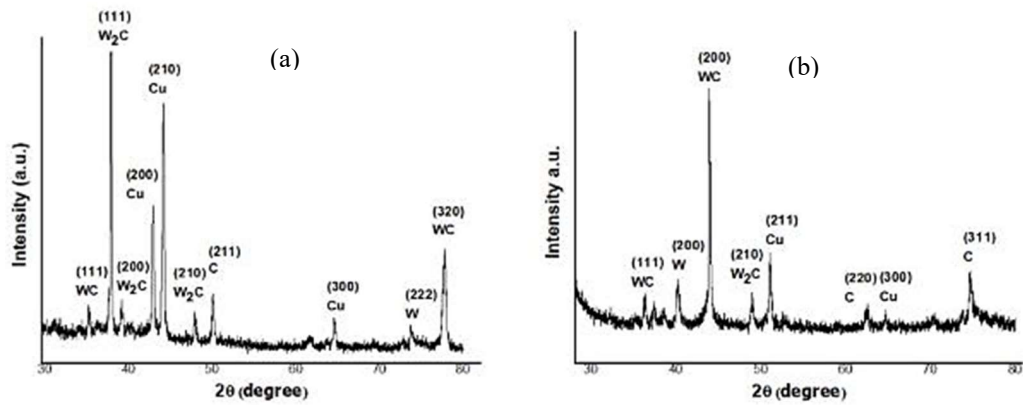
Figure 2.21 Material that observed deposited on the coating layer by using XRD analysis with different current applied a) 6 A b) and 8 A (Mazarbhuiya et al., 2020).

Tijo & Masanta (2017) conducted an XRD analysis to examine the element that deposited on Ti-6Al-4V alloy surface. With a peak current is 5 A and the duty factor is varying from 70, 75 and 80%, it is found that the major element that presence in the coating layer of Ti-6Al-4V alloy workpiece surface is titanium carbide (TiC), titanium boride (TiB) and titanium diboride (TiB$_2$). The presence of TiC and TiB$_2$ is due to the reaction between Ti and boron carbide (B$_4$C) powder that added into the dieletric fluid during EDC process. While, the presence of TiB is due to the incomplete reaction between Ti and B$_4$C powder. In the other hand, an element such as Ti, TiO$_2$ and C also observed present on the surface of coating layer. Figure 2.22 shows the XRD profiles of element that deposited on Ti-6Al-4V alloy workpiece surface after EDC process.
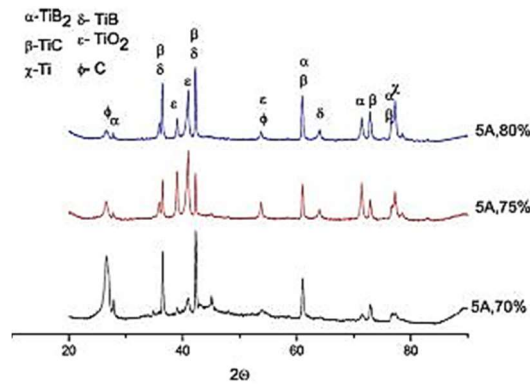
Figure 2.22: XRD profile of element composition on Ti-6Al-4V alloy workpiece surface after EDC process (Tijo & Masanta, 2017).

A recent research by Patowari & Mussada (2017) observed that, the presence of elements such as tungsten (W), Iron (Fe), copper (Cu) and the carbides of Fe and W is found on the coating surface after stepwise machining conducted. The presence of this element is detected by using XRD analysis. The production of this elements is due to reaction during the discharge energy between the carbon that contain in the hydrocarbon oil and the W-Cu powder that contained in the P/M electrode with composition 75%: 25%. Figure 2.23 shows the element that that exist on the coating layer surface.
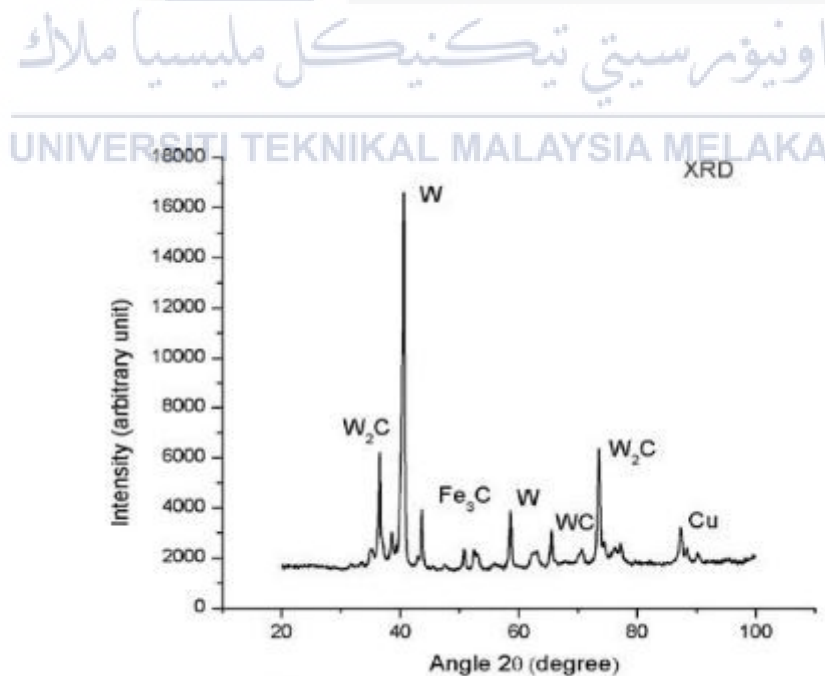
Figure 2.23: The existence of element that deposited on the coating layer that detected by using XRD analysis after stepwise machining (Patowari & Mussada, 2017).

Liew et al. (2018) reported that there are five elements that found deposited on the aluminium surface which contain carbon, aluminum, tungsten, oxygen and copper. The presence of carbon that produce from kerosene oil is due to the high temperature that applied during the EDC process where it is essential. Aluminum and copper come from the tool electrode that eroded during EDC process and also from the workpiece itself while the presence of oxygen is due to the cooling process where oxygen is absorbed into the deposition layer since it is exposed to atmosphere after EDC process.

2.6.4 Corrosion Resistance

Resistance of corrosion refers to the resistance of the material to adverse reactions that may corrode the material. Corrosion is a process in which the material is oxidized by substances in the environment which cause the material to lose electrons (Janssen, 2019). According to Olsen (2020), corrosion may develop in the presence of liquids or gases. It may occur at any temperature, although, in general, the rate of corrosion increases with rising temperatures.

Toshimitsu et al. (2016) reported that the corrosion resistance can be evaluated by using electrochemical analysis system. The schematic view of electrochemical analysis system can be seen in Figure 2.24 below. In this research, negative polarity is used in the EDM machine to coat the alloy steel workpiece where chromium (Cr) powder is added into the dielectric fluid and copper is used as an electrode. As a result, the usage of Cr powder definitely can increase the corrosion resistance of the workpiece since the resolidified layer containing Cr powder is uniformly formed as a coating layer.
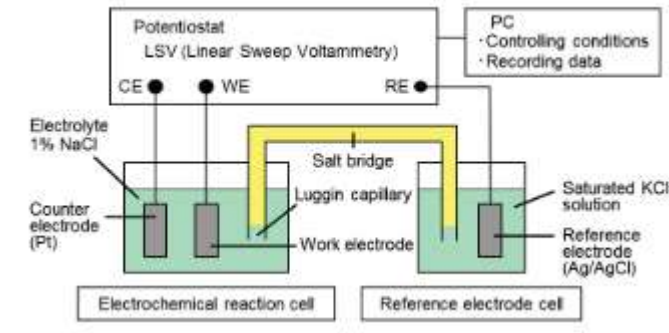
Figure 2.24: Schematic view of electrochemical analysis system (Toshimitsu et al., 2016).

Sumi et al. (2011) reported that the corrosion resistance can be evaluated by using aqua regia dip test. In this test, the coated workpiece is immersed in aqua regia solution. The result shows that the worpiece area which contain Si-containing amorphous layer does not corrode compared to workpiece area without Si-containing amorphous layer that corroded by 0.15 mm. in the other hand, it is observed that a lot of bubbles is found on the non-coated area while it is vice versa for coated area. This shows that, the existence of Si-containing amorphous layer is proved can provide a protective layer on the workpiece by using EDC process.

Sharma et al. (2020) using PMEDM as process to coat the workpiece of titanium alloy while brass was used as a tool electrode. Reverse polarity is applied and the powder added into the dielectric fluid is hexagonal boron nitride (hBN) with size particle 70nm. The value of voltage (20, 40 and 60 V), duty factor (0.3, 0.5 and 0.7) and powder concentration (6, 8, 10 and 12 g/L) are varied. The result shows that, at the parameter of 60 V and 0.5 duty, in stagnant condition, it can be seen in Figure 2.25 that the corrosion rate is decreased when the powder concentration is increase. A high concentration of hBN powder added increased the corrosion resistance of the workpiece. In flowing condition, three different rpm is applied with the value of 500, 1000 and 1500 rpm. The result is same as stagnant condition where the deposition rate is decrease when the concentration is increased and the effect of rotary spindle is insignificant. Figure 2.26 shows the effect of powder concentration along with spindle rotary with the corrosion rate.
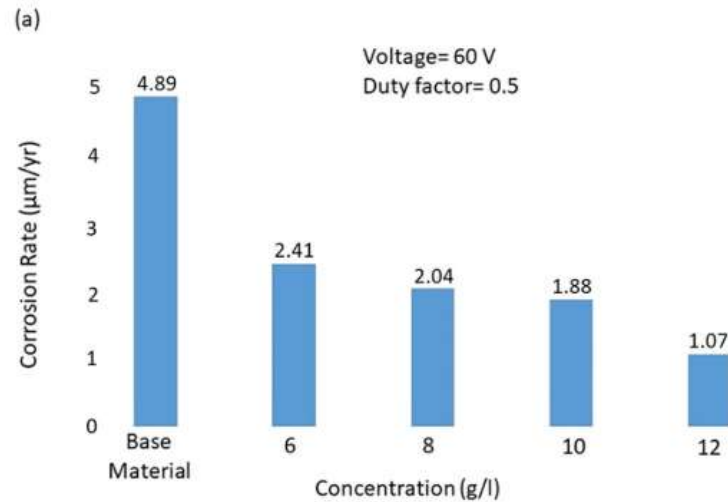
Figure 2.25: Relationship between concentration of powder with corrosion rate (Sharma et al., 2020b).
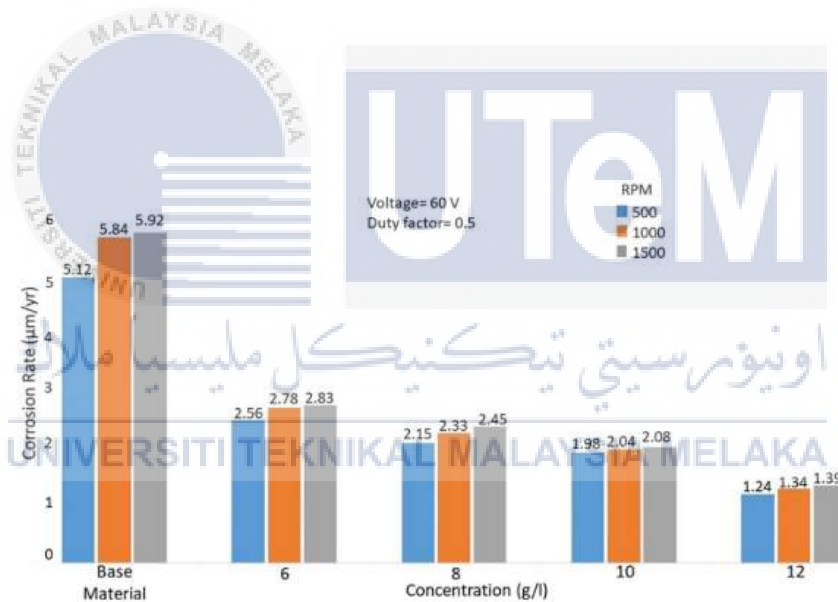
Figure 2.26: The effect of powder concentration along with spindle rotary with the corrosion rate (Sharma et al., 2020b).

Prakash et al. (2015) shows that PMEDM not only help to improve the surface hardness but also provide a protective layer on the specimen surface to prevent corrosion. The deposition of bioceramic-oxide layer act as barrier to prevent corrosion thus increase the corrosion resistance. In Table 2.5, it can be seen that the difference between the PMEDM-machined and non-machined specimen which gained by using Tafel extrapolation method

shows a high value of corrosion with value 101 nA/cm^2 compared to machined specimen where the value is 41 nA/cm^2.

Table 2.5: Corrosion parameter of non-machined and PMEDM machined specimen (Prakash et al., 2015).

Parameters	β – Ti alloy specimens	
	Non- machined	PMEDM -machined
Icorr (nA/cm^2)	101	41
Ecorr (mV vs. SCE)	-79.76	-342.47
Rp (Ω cm^2)	16 328	280 250
CR (mm/year)	0.00117	0.00047

2.6.5 Wear resistance

Wear is characterized as the loss or deformation of a metal resulting from mechanical interaction with a specific material. Wear may take various forms including abrasion, adhesion or galling, erosion, and spalling which commonly measured as the amount of mass lost in a given time. It can be said that temperature and the fluid environment also affect the rate and types of wear (Olsen, 2020). According to Chakraborty et al. (2018), many researches have been done and EDC process not only can enhance the surface hardness of the material but also provide a wear resistance coating on the material.

Sharma et al. (2020) revealed that the addition of hBN powder into the PMEDM process provided high wear resistance of the titanium alloy workpiece. Pin on disk wear test with a constant value of wear disk rpm at 400 rpm, 1 kgf of dead load and the time duration is 15 minutes was conducted on titanium alloy coated with hBN and non-coated titanium alloy (base material). The result shows that the wear rate of workpice that coated with hBN is reduce from 0.19 mg/min to 0.05 mg/min as the duty factor is increased as can be seen in Figure 2.27. Whereas, the value of wear rate of base material shows a higher value which is 0.22 mg/min.
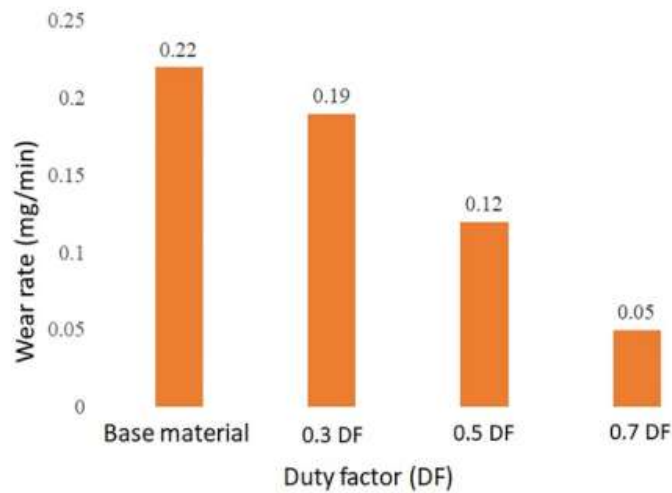
Figure 2.27 : Effect of duty factor on value of wear rate for base material and hBN coated material (Sharma et al., 2020a).

Sumi et al. (2011) compared the friction coefficient and wear properties of SKD II without coating layer and SKD II with Si-containing amorphous layer that machined by using EDC process. The result shows that Si-containing amorphous layer have a lower value of friction coefficient which is 0.35 approximately while the value of friction coefficient for SKD II without coating layer is 0.8. Since the value of friction coefficient of Si-containing layer is low, the ratio wear amount also low. This proved that the wear resistance of Si-containing amorphous layer is high. This happen because the properties of the coating layer are hard and smooth. Figure 2.28 shows the value of wear ratio for both workpiece where it can be seen that the difference amount of wear ratio is significant.
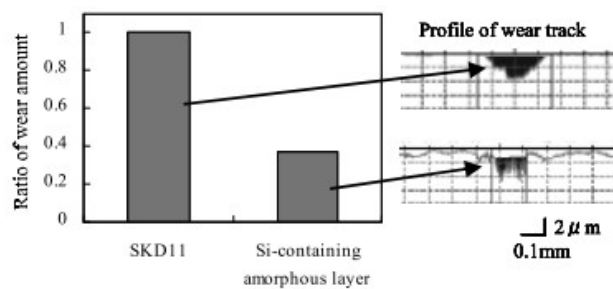
Figure 2.28: Wear ratio of SKD II and Si-containing amorphous layer (Sumi et al., 2011).

Ueno et al. (2016) investigated the wear characteristic of steel sheet roll surface that coated with TiC by using EDC process and conventional chrome-plated rolls. They found that the wear resistance of sheet rolls coated with TiC is high compared to conventional chrome-plated rolls. Ueno et al. (2016) also stated that, to achieve a high wear resistance of deposited layer, a suitable parameters in EDC process need to be applied.

2.7 Aluminium

Aluminum is one of the most abundant compound that commonly found in the earth crust. However, it is impossible to found the aluminum in a pure form. Generally, aluminum will react with oxygen readily and the ore is known as bauxite. To separate the other element and impurities that contained in the bauxite, the raw rock is crushed and dried to remove the water then electrolysis technique is used to separate the aluminum and oxygen (Woodford, 2020).

In 1809, Sir Humphry Davy found the aluminium, but unfortunately he is unable to separate the aluminum from other elements. However, in 1827, Friedrich Wohler, a chemist form Germany success to separate the aluminium by heating it with potassium metal. Two chemist in United States, Charles Martin Haul and Paul Louis Toussant Herolts then found another technique called as electrolysis or also known as Hall Heroult process to separate the aluminium in 1886 and make the price of aluminium dropped from 12 to 4 dollars. In order to produce a large quantity of aluminium, an Austrian Chemist, Karl Bayer add Bayer process to refine the alumina and electrolysis was used to smelted alumina into pure metal aluminium and this technique still used until nowadays (Laparra, 2012).

Table 2.6: Properties of aluminium (Azom, 2020).

GENERAL PROPERTIES	
Density	2.5×10^3 - 2.9×10^3 kg/m³
MECHANICAL PROPERTIES	
Yield Strength	3×10^7 - 5.0×10^8 Pa
Tensile Strength	5.8×10^7 - 5.0×10^8 Pa
Elongation	0.01 - 0.44 % strain
Hardness (Vickers)	1.18×10^8 - 1.48×10^9 Pa
Impact Strength (un-notched)	1.9×10^5 - 2.0×10^5 J/m²
Fracture Toughness	2.27×10^7 - 3.5×10^7 Pa/m$^{0.5}$
Young's Modulus	6.8×10^{10} - 8.2×10^{10} Pa
THERMAL PROPERTIES	
Max Services Temperature	120 - 210 °C
Melting Temperature	475 - 677 °C
Insulator or Conductor	Good Conductor
Specific Heat Capability	857 - 990 J/kg °C
Thermal Expansion Coefficient	2.1×10^{-5} - $2..4 \times 10^{-5}$ Strain/°C
ELECTRICAL PROPERTIES	
Electrical Resistivity	2.5×10^{-8} – 6.5×10^{-8} °C
ECO	
CO_2 Footprint	1.85-204 kg/kg
Recycleable	Yes

In industry, aluminium is in high demand due to its unique characteristic. Lightweight, corrosion resistance and low cost make aluminium always be the first choice to create a product especially in aerospace and automotive industry (Stojanovic et al., 2018). However, according to Chi et al. (2018), aluminium has poor wear resistance and poor hardness, then by adding alloying element in it will improve its properties. There are seven series of wrought designation system. Table 2.7 shows the difference between the elements of alloy that consist in the aluminium together with its application.

Table 2.7: Seven series of wrought designation system with its application(Alcotec, 2020).

Alloy Series	Alloying Element	Application
1xxx	Aluminium (99%)	Pipeline, chemical tanks, aluminium foil, wire
2xxx	Copper	Wire, armor plate, fasteners, aircraft and body truck.
3xxx	Manganese	Heat exchanger (automotive and plant), beverages can and cooking utensil.
4xxx	Silicon	Filler material for welding, and aircraft piston
5xxx	Magnesium	Building infrastructure, bridge, storage tanks, body panel and frame (automotive) and marine.
6xxx	Magnesium and Silicon	Bridge structure, building infrastructure, frames (truck and marine) and pipeline.
7xxx	Zinc	Aircraft industry.

2.8 Research Gap and Summary

Based on the previous research that has been done by previous researcher, Table 2.8 shows the summary of the related journal or article. The parameter and the result gained from each experiment are shown in the table:

Table 2.8: Summary of related journal and article.

Author	Technique used	Parameter	Objective	Result
Janmanee & Muttamara (2012)	PMEDM	Electrode: Copper Workpiece: Tungsten Carbide Powder addition: Titanium (Ti) Polarity:Negative Current (A): 10, 15, 20, 25 Voltage (V):1 50 Pulse on time (μs):510 Pulse off time:- Powder concentration (g/L): 50 Duty factor (%): 20, 40, 50, 80	To study the thickness of layer, surface hardness and chemical composition on the wokrpiece surface after EDC process with powder suspension of Titanium	The surface hardness is increase. Microcrack reduce. Enhancement in quality of modified surface.

43

Author	Method	Parameters	Objective	Findings
Kumar & Batra (2012)	PMEDM	Electrode: Copper Workpiece: Die steel (3 different die steel) Powder addition: Tungsten carbide Polarity: Negative Current (A): 2, 4 ,6 Voltage (V): not stated Pulse on time (μs):-5, 10, 20 Pulse off time:2,4,6 Powder concentration (g/L): 15 Duty factor (%): -	To investigate the reaction of three different die steel workpiece when tungsten is added into the dielectric fluid.	Tungsten carbide is deposited on the workpiece surface shows that EDM with reversed polarity is possible to coat the material. Increase in micro hardness
Kudilil et al. (2012)	Melt mixing	Weight percentage of TiO_2 (%): 0-3	To investigate the effect of TiO_2 as an additive in polypropylene.	Tensile strength and modulus is increased as the weight percentage is increased. Elongation at break increase after thermal ageing. Thermal stability of PP is increase as the weight percentage is increased.
Tijo & Masanta (2012)	EDC with PM electrode	Electrode: Tungsten and Copper PM Workpiece: Aluminium Powder addition: - Polarity: Negative Current (A): 2,3,4 Voltage (V): not stated Pulse on time (μs): 100, 200, 300 Pulse off time (μs):- Tool compaction pressure (MPa): 150, 200, 0 Duty factor (%): -	To study the effect of compaction pressure of tool coated with tungsten and copper by PM method with the peak current and pulse on time.	A high compaction pressure reduced the tool wear rate and material deposition. Relate with the increment of peak current and pulse on time the TWR and material deposition is increased.

Watane (2017)	EDC with PM electrode	Electrode: Tiatnium carbide and copper (TiC-Cu) Workpiece: Mild steel Polarity: Negative Powder proportions (TiC:Cu): 30:70, 50:50, 70:30 wt.% Compaction pressure: 150, 200 and 250 MPa Current (A): 2,4 Voltage (V): - Pulse on time (µs): - Pulse off time (µs): - Powder concentration (g/L): - Duty factor (%):-	To identify effect of different compaction pressure and composition of tool electrode on surface hardness of mils steel.	The usage of TiC-Cu tool electrode increase the micro hardness of the workpiece and the deposition rate is higher when low compaction pressure is applied on the tool electrode. A high composition of Ti also help in rate deposition of the tool electrode along with the increment of peak current.
Jemat et al. (2017)	Plasma sprayed	Weight percentage of TiO2 (%) : 0, 10, 20, 30	To study the effect of yttria stabilised zirconia (YZP) with addition of TiO2 powder in plasma sprayed method.	The reduction of crack can be seen at the same time increase the hardness. The increment in weight percentage of TiO_2 increase the adhesion strength.

Author	Method	Parameters	Findings
Liew et al. (2018)	PMEDM	Electrode: Copper Workpiece: Aluminium 6061 Powder addition: Tungsten Polarity: Negative Current (A): 3, 4, 5 Voltage (V): 20, 25, 30, 35, 40 Pulse on time (μs):150,200,250 Pulse off time (μs):-20 Powder concentration (g/L): 8 Duty factor (%):-	The investigate the effect of pulse on time, peak current and voltage on the surface topography, surface hardness and weight percentage of elemental composition after EDC process. There are another element is observed on the workpiece and the micro hardness of the surface is increased. The optimum parameter that identified is: Peak current: 3A Pulse on time : 150 μs Voltage: 40 V
Panda (2019)	PMEDM	Electrode: Copper and graphite Workpiece: AISI D3 Powder addition: Manganese Polarity: Negative Current (A): 4,6,8 Voltage (V) : not stated Pulse on time (μs): 21, 50, 100 Pulse off time (μs):20, 40, 75 Powder concentration (g/L): 5, 10, 15 Duty factor (%): -	To study the effect of manganese powder addition in EDC process on the AISI D3 surface hardness The micro hardness of the AISI D3 workpiece is increased.
Shyam Kumar et al (2019)	Wet mixing	Weight percentage of TiO2 (%): 2,4,6	To investigate the effect of TiO2 as an additive in production of porous mullite ceramic on its mechanical properties. The strength and densification is improved when TiO$_2$ is added. The porosity of the ceramic also reduced.

| Sharma et al. (2020) | PMEDM | Electrode: Brass
Workpiece: Titanium alloy
Powder addition: hexagonal boron nitride (hBN)
Polarity: Negative
Current (A): -
Voltage (V): 20, 40, 60
Pulse on time (µs): -
Pulse off time (µs): -
Powder concentration (g/L): 6, 8, 10, 12
Duty factor (%): 3,5,7 | To study the influence of input parameter on wear properties, corrosion properties and the surface integrity. | The micro hardness of the workpiece surface is increased. The material deposition rate is achieved 5.65 ± 0.1×10−4 g/min and the thickness layer obtained is 13.1 µm. The wear rate of coated layer is reduced.
Optimum parameter:
Voltage: 60
Duty factory (%): 7
Powder concentration (g/) : 12 |

From the Table 2.8, PMEDM is proved can be used to create a coating layer on the workpiece as a protective layer which can improve its hardness. Although aluminium already has a good wear and corrosion resistance, after some duration of time, it will corrode and wear due to exposure to high temperature, pressure and loads along the operation. It is crucial to find a way to increase its lifespan.

On the other hand, the usage of W in automotive, military and cutting tool also attract the attention of few researchers to further the investigation of W by using various techniques and application. Many studies have explored the effect of powder as an additive in in EDC process, however, tungsten powder has not been used yet. Therefore, this research was conducted by using W as a powder material in PMEDM process to modify the surface of aluminium 6061.

CHAPTER 3
METHODOLOGY

In this chapter, experimental information including the equipment, material preparation and the experimental procedure were described. In order to fulfill the objectives of the research, the experiment was conducted with a suitable method, tools and technique.

3.1 Gantt chart

Gantt chart is one of tool that used in project management for planning and schedule the activity of the project. In this research, this tool was used to monitor and track the activity of the research to ensure the research is run smoothly. The gantt chart was shown in appendix.

3. 2 Flow Chart

Flow chart is used to organize the experimental procedure for the research. For this research, the flow chart can be seen in Figure 3.1.
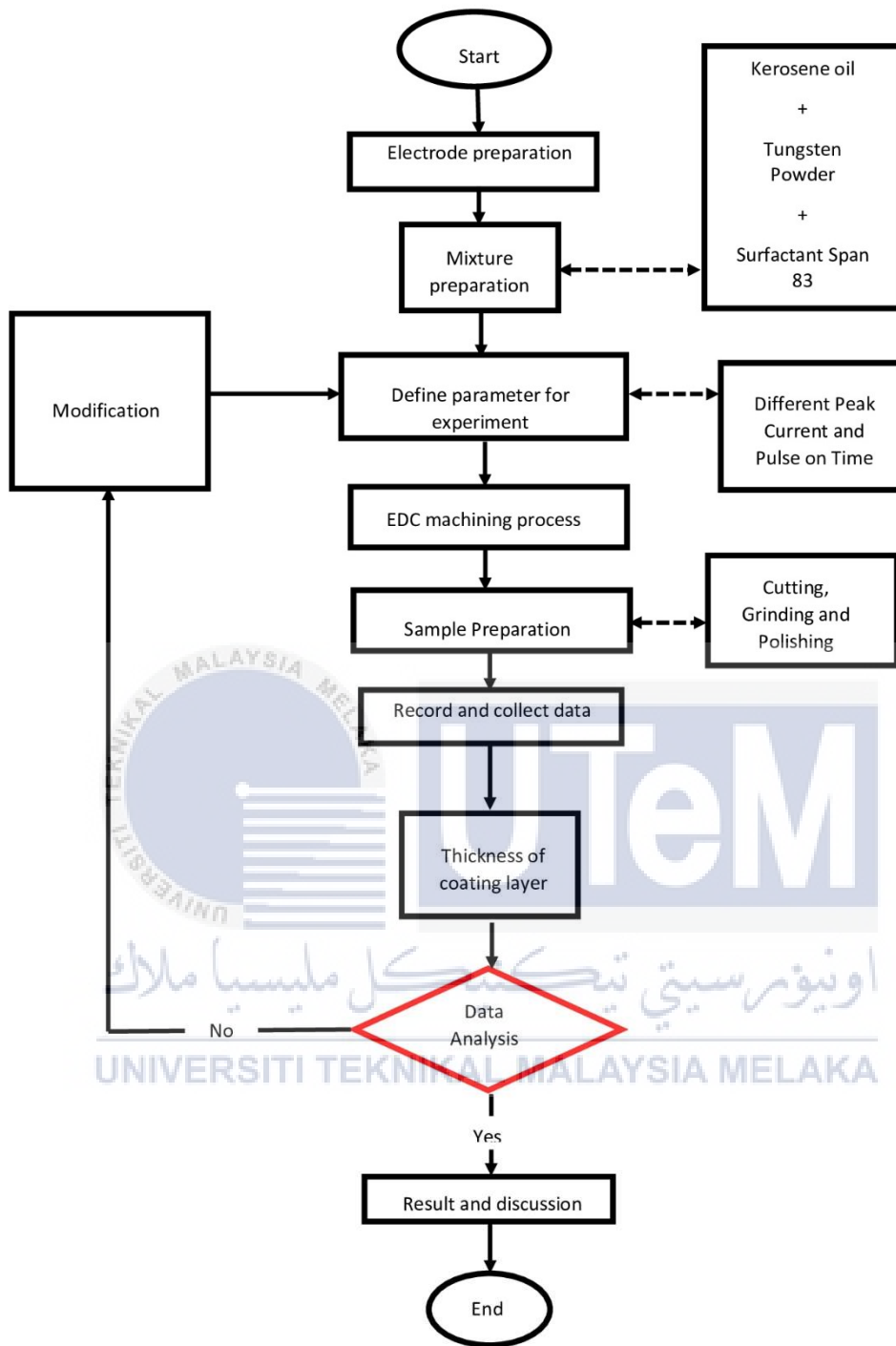
Figure 3.1: Methodology flow chart.

3.3   Equipment and Material Preparation

In order to run the EDC process, suitable equipment was selected and all the material preparation was done before experiment.

3.3.1   Machine

A die sinking machine of Sodick AQ35L was used to conduct EDC experiment. This die sinker machine consists of 3 axis (X, Y, Z) linear motor drive system with a quick response and vibration free servo system and using 3 micro chuck system. The maximum power supply machining current is 40 A. The machine provides inner tank with dimension width 750 mm, length 500 mm height 320 mm, and the maximum capacity of the tank can reach 112 L. The level adjustment of the machining table for x axis (left and right) is 350 mm, y axis (front and rear) is 250 mm, and z axis (up and down) 250 mm. On the other hand, this machine can hold a maximum weight of workpiece up to 550 kg whereas the maximum weight of electrode up to 50 kg. Figure 3.2 shows the image of Sodick AQ35L die sinker EDM machine.

Figure 3.2: Sodick AQ35L Die Sinker EDM machine.

3.3.2 Workpiece

In this research, aluminium 6061 was used as a workpiece material with the dimension of 30 mm x 50 mm x 15 mm. Figure 3.3 shows the image of aluminium 6061workpiece. Table 3.1 shows the mechanical properties of aluminium 6061 while table 3.2 shows the chemical composition of aluminium 6061.

Figure 3.3: Aluminium 6061 workpiece.

Table 3.1: Mechanical properties of aluminium 6061 (Nunes et al., 1990).

Properties	Values
Melting Temperature, Tm (°C)	582 - 652
Density, g/cm^3	2.7
Young Modulus, E (Gpa)	68.9
Tensile Yield Strength, σ_y (MPa)	276
Ultimate Tensile Strength, σ_s (MPa)	310
Fatigue Strength, S$_{Nf}$ (MPa)	96.5
Hardness, Brinell (BHN)	95 kgf/mm^2
Hardness, Knoop (HK)	120 kgf/mm^2
Hardness, Rockwell (HRC)	60 kgf/mm^2
Hardness, Vickers (HV)	107 kgf/mm^2

Table 3.2: Composition of chemical in aluminium 6061 (Nunes et al., 1990).

Element	Content (%)
Aluminium, Al	97.9
Magnesium, Mg	1
Silicon, Si	0.60
Copper, Cu	0.28
Chromium, Cr	0.20

3.3.3 Tool Electrode

Copper was selected as tool electrode in this research, as shown in Figure 3.4. The dimension of the copper electrode is 6 mm diameter and 78 mm in length. Before the tool electrode was used for the experiment, the base of the electrode was grinded by using 320 grit sand paper with 300 rpm in order to get a flat base surface. Table 3.3 shows the properties of copper tool electrode.

Figure 3.4: Copper electrode.

Table 3.3: Main properties of copper electrode (Teimouri & Baseri, 2012).

Properties	Description
Specific Gravity (G/Cm^3)	8.94
Melting Range (°C)	1065 - 1083
Thermal Conductivity (W/ Mk)	388
Specific Heat (J/Kgk)	385
Thermal Expansion Coeffcient (1/°C)	16.7 x 10 -6
Electrical Resistivity (Ω Cm)	1.7 x 10 -6

3.3.4   Preparation of Mixture

Before the experiment begin, the type of surfactant need to be determined first. Commonly, to identify whether the surfactant is suitable or not with our selected powder, the dielectric fluid, surfactant and powder material need to be mixed and stirred together by using ultrasonic homogenizer machine. To dilute the powder, surfactant and kerosene oil, equation 3.1 was used to calculate the concentration of mixture. After a few days of observation, when less precipitate of powder was observed in the dielectric fluid, it indicates that the surfactant used is suitable. The importance of surfactant is to help the powder to disperse well with the dielectric fluid and to avoid the agglomeration of the powder at the bottom of EDC tank. In this research, Span 83 that manufactured by Sigma-Aldrich (M) Sdn Bhd was selected. Figure 3.5 shows the flow chart for the selection of surfactant and Table 3.4 shows the properties of surfactant Span 83.

$$\text{Concentration of mixture (g/L)} = \frac{\text{Powder Weight (g)}}{\text{Volume of dielectric Fluid (L)}} \quad \text{... Equation 3.1}$$
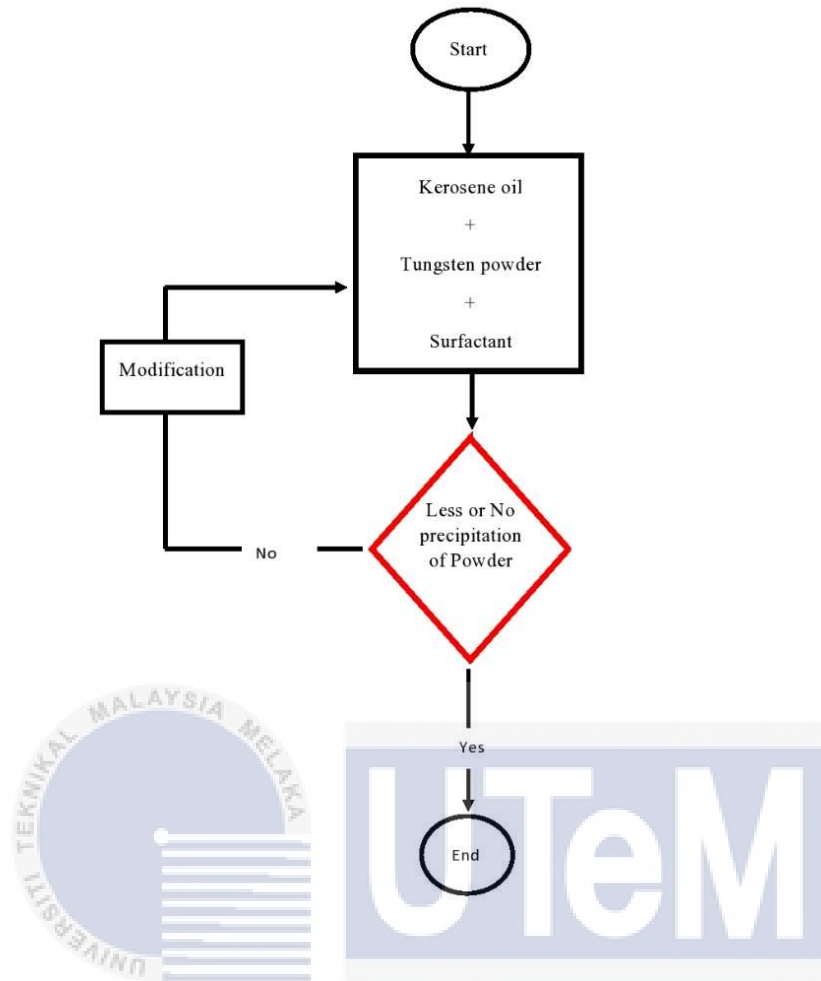
Figure 3.5: Flow chart for selection of surfactant.

Table 3.4: Properties of surfactant Span 83 (Sigma Aldrich (M) Sdn.Bhd).

Properties	Value
Chemical Formula	$C_{33}H_{60}O_{0.5}$
Molecular weight (g/mol)	561.00
Vapor Pressure (20°C)	0.81 Psi
Refractive Index	n20/D 1.478 (lit)
Density (25°C)	0.989 g/ml
Flash Point	113 °C
HLB	3

Tungsten powder that manufactured by KFO French Co., Ltd with the purity of 99.5% was used as an additive powder into the dielectric fluid for the EDC process in this research. Figure 3.6 shows the image of tungsten powder used with the average of particle size is 1.29 μm. According to Dvoracek et al. (2018), in automotive, electrical and military, the usage of tungsten is widespread due to its high melting point and strength. Many research have been done and it is proved that the usage of tungsten powder can enhance the mechanical properties. Table 3.5 shows the properties of tungsten powder with purity 99.5% that manufactured by KFO French Co., Ltd.

Figure 3.6: Tungsten powder (KFO French Co., Ltd).

Table 3.5: Properties of tungsten powder (KFO French Co., Ltd).

Properties	Values
Density (g/cm)	19.35
Melting point (ºC)	3410 ± 20
Boiling point (ºC)	5927

Dielectric fluid act as an agent to flow the debris of eliminated material of the workpiece away from the spark gap area. It also functions as a coolant where dielectric fluid remove heat from the tool electrode, workpiece and spark area. On the other hand, dielectric fluid also deionized the spark gap after the discharge. In this research, EDM low smell kerosene oil that manufactured by Global Work Co. Ltd was used as a dielectric fluid. Kerosene oil was selected as dielectric fluid because it is commonly used in EDC process. On the other hand, the long chain of carbon in kerosene oil with the formula of

$C_{12}H_{26}-C_{15}H_{32}$ also will help in the enhancement of surface hardness once the carbon chain is decomposed and deposited on the workpiece surface.

To run the EDC process, 8 gram of tungsten powder and Span 83 were added into 500 ml of kerosene oil for about 5 minutes to ensure the powder dissolve well, while another 30 minutes was taken to mix all the mixture by using Labsonic Ultrasonic Homogenizer Type p Series as can be seen in Figure 3.7, with the amplitude 50% and the interval was 0.5.
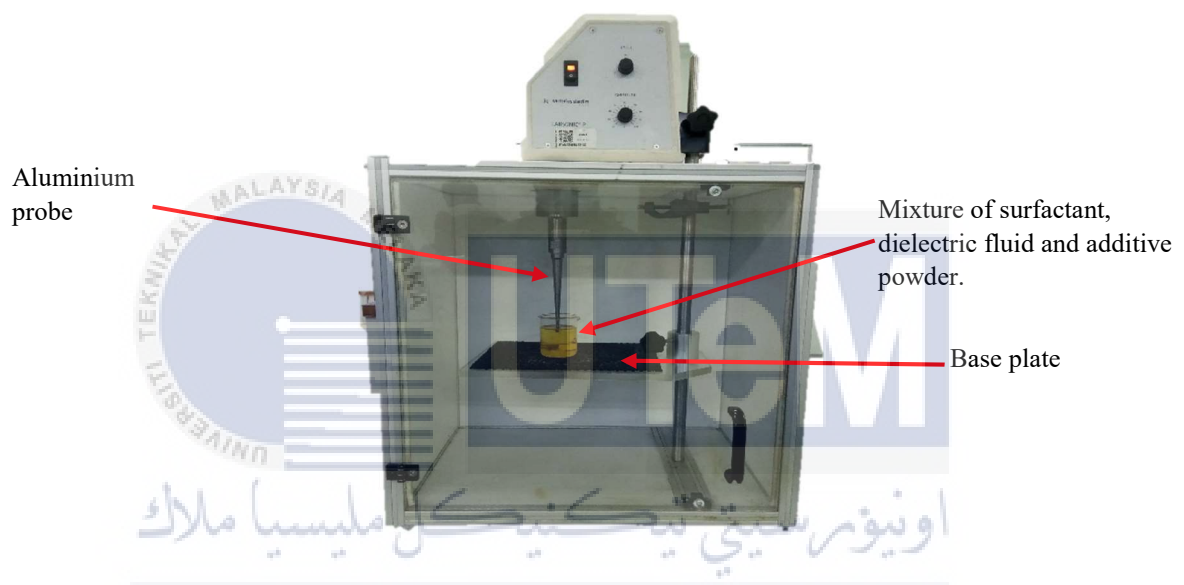
Figure 3.7: Labsonic Ultrasonic Homogenizer type P Series (Tribology laboratory, FKM UTeM).

3.4 Experimental Procedure

Before the experiment start, the electrode was dressed first to gain a flat surface at the end of the electrode. With the help of grinding and polishing machine from Buehler International Inc, the flat surface was gained and the burrs was removed from the end of electrode. Figure 3.8 shows the grinding and polishing machine that was used in FKP UTEM laboratory to dress the electrode.

Figure 3.8: Grinding and polishing machine (FKP UTeM laboratory).

In the EDC experiment, the polarity was reversed, where aluminium 6061 workpiece placed at negative terminal and copper electrode placed at positive terminal. Electrode copper was mounted tightly on the electrode holder altogether with the drill chuck while the aluminum workpiece was clamped tightly at the stainless steel jig to avoid reposition of workpiece and tool electrode during machining process. Then, the flushing system was set up and the mixture of kerosene oil was poured into the EDM machine dielectric fluid tank.

The time for the EDM machine to operate was set to 30 minutes for each experiment. The peak current and pulse on time were varied with the value of 3A and 4A and 150, 200 and 250 μs respectively, while the other parameters such as voltage, pulse of time and machining time were kept constant. Table 3.6 shows the parameter and experiment conditions for the process. After the process end, the aluminium 6061 workpiece and copper electrode was taken out from the EDM machine and cleaned by using air gun to remove dielectric oil and debris that attached on it. Lastly, the aluminium 6061 material was analyzed to gain the result for thickness of deposited layer.

Table 3.6: Parameter and experiment condition of EDC process.

Workpiece Material	Aluminium 6061
Tool Electrode	Copper
Dielectric Fluid	Kerosene Oil
Powder Materials	Tungsten
Polarity	Aluminum 6061 Workpiece - Negative Copper Electrode - Positive
Powder weight	8 g
Span 83 weight	8 g
Voltage	40 (V)
Current	3 and 4 (A)
pulse on time	150, 200 and 250 μs
Pulse off time	20 μs
Machining Time	30 minutes

3.5   Measurement and analysis

In this subtopic, the method of collection of data and the measurement and analysis to identify the micrograph of W powder and thickness of coating layer were explained.

3.5.1 Morphology and particles size of W powder

The morphology of W powder was investigated by using SEM machine model Zeiss EVO 50 to identify the shape of W powder and the average particle size, W powder was dispersed by using ultrasonic bath for about 30 minutes with the highest vibration. A small amount of dispersed powder then poured on the carbon tape of SEM stub holder and ready for imaging. Figure 3.9 shows the SEM holder with the W powder on it.
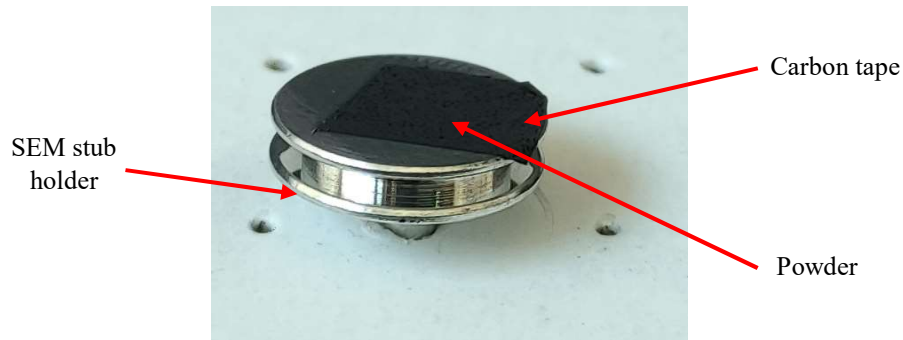
Figure 3.9: W powder on SEM stub holder.

3.5.2 Coating layer

To gain the data for thickness of deposited layer, the workpiece was cut into small pieces by using Miracut 151 Low Speed Precicion Cut off Machine with 4 inches diamond wafering blade with speed 190 rpm. Figure 3.10 shows the image of Miracut 151 Low Speed Precicion Cut off Machine with its part function. After the cutting process done, the workpiece then immersed into the ethanol solution and was placed in the ultrasonic bath with higher level of vibration for about 5 minutes to remove the debris from cutting process. Figure 3.11 shows the ultrasonic bath that was used in FKP Utem laboratory.
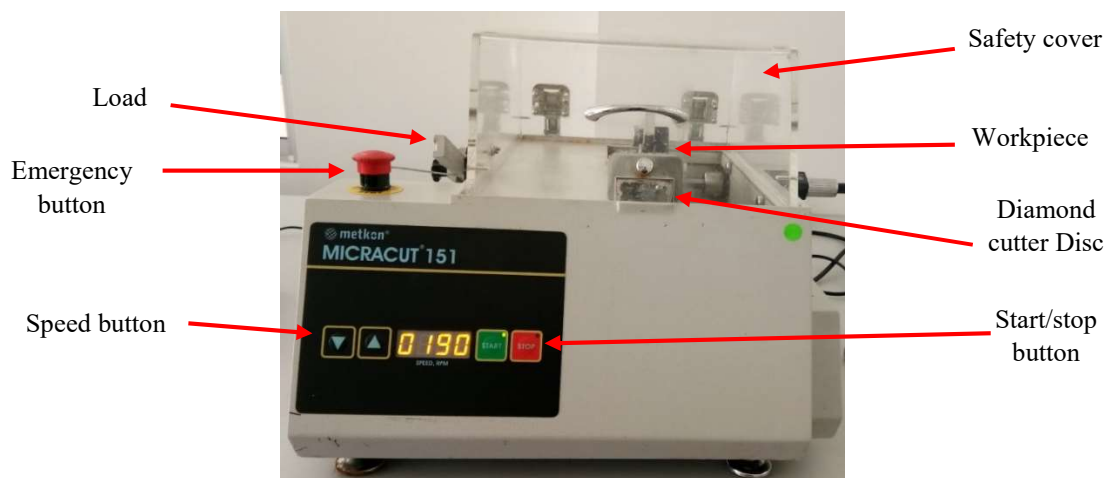
Figure 3.10: Miracut 151 Low Speed Precicion Cut off Machine with 4 inches diamond wafering blade (FKP UTeM Laboratory).

Figure 3.11: Ultrasonic bath Powersonic 410 (FKP UTeM Laboratory).

Once the aluminium 6061 workpiece was cleaned, grinding process was done by using 600, 800 and 1200 grit sand paper to remove the burr and to gain a smooth surface at the cross section area. While to gain a mirror surface at the cross section area, polishing process was done by using 1.0 µm diamat polycrystalline diamond suspension and 0.05 µm nanopolish alumina suspension that was manufactured by PACE Technologies Corporation as can be seen in Figure 3.12.

(a)   (b)

Figure 3.12: Final polishing abrasive (a) 1.0 µm diamat polycrystalline diamond suspension (b) 0.05 µm nanopolish alumina suspension.

61

Once the sample preparation was finish, the thickness of the deposited layer was observed from the cross sectional cut by using SEM machine model Zeiss EVO 50. SEM images on samples processed at higher magnifications of the deposited layer. Figure 3.13 shows the SEM machine model Zeiss EVO 50.

Figure 3.13: SEM machine model Zeiss EVO 50.

CHAPTER 4

RESULT AND DISCUSSION

This chapter shows the result of each sample that has been tested and analyzed. The result gained was discussed and supported by previous research on the relationship between the effect of pulse on time and peak current with the thickness of coating.

4.1 Micrograph of Tungsten (W) Powder

To gain the micrograph of tungsten powder, Scanning Electron Microscopy (SEM) machine model Zeiss EVO 50 was used. Figure 4.1 shows the image of tungsten powder with purity of 99.5% that was taken with magnification of 10000X. It can be seen that the shape of tungsten powder is in irregular shape. Same pattern of shape also were taken by Kanpara et al. (2014) and Rodriguez et al. (2011) in their research where they observed that the shape of the tungsten powder is not in spherical and faceted shape. From the SEM images, the average particle size that were gained is $\bar{x} = 1.29$ µm. To get the average value of the particle size, 10 measurement were taken from different particle. The measurement and calculation for the average particle size can be seen in appendix. According to Abdudeen et al. (2020), the size of particle that commonly used in EDC is 1 to 50 µm and 20 to 150 nanometer. The importance to identify the size of particle is to gain a suitable size that commonly used in EDC process and to prevent short circuit during the EDC process that caused by a large size of particle that block the gap between the electrode and workpiece.
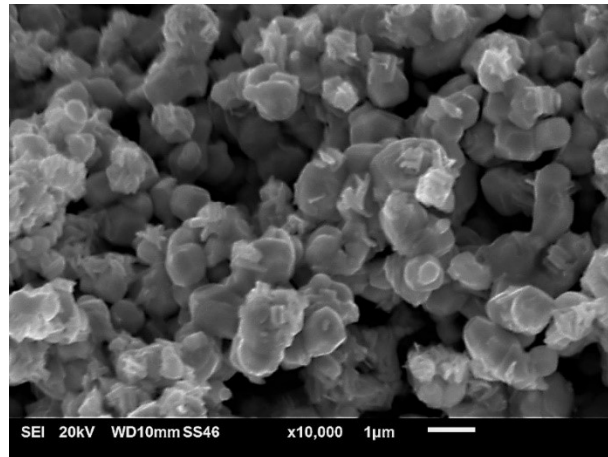
Figure 4.1: Micrograph of tungsten powder.

4.2   Thickness of Coating Layer

The thickness of coating layer on aluminium 6061 workpiece was investigated for each different parameter. Figure 4.2 shows the image of SEM analysis of the aluminium workpiece coated with tungsten powder with magnification of 2000X at the cross section area. 10 measurements of coating layer thickness were taken at different spot by using SEM to identify the average of coating thickness. The calculation and each measurement was shown in appendix. From the Figure 4.2, it can be seen that the tungsten powder deposited uniformly on the aluminium 6061 workpiece with different thickness. The thinnest coating layer thickness was obtained by using peak current at 3A with pulse on time 150 μs and the thickest was obtained by using 4A of peak current with pulse on time 250 μs. Table 4.1 shows the data of average thickness of coating layer for each parameter.
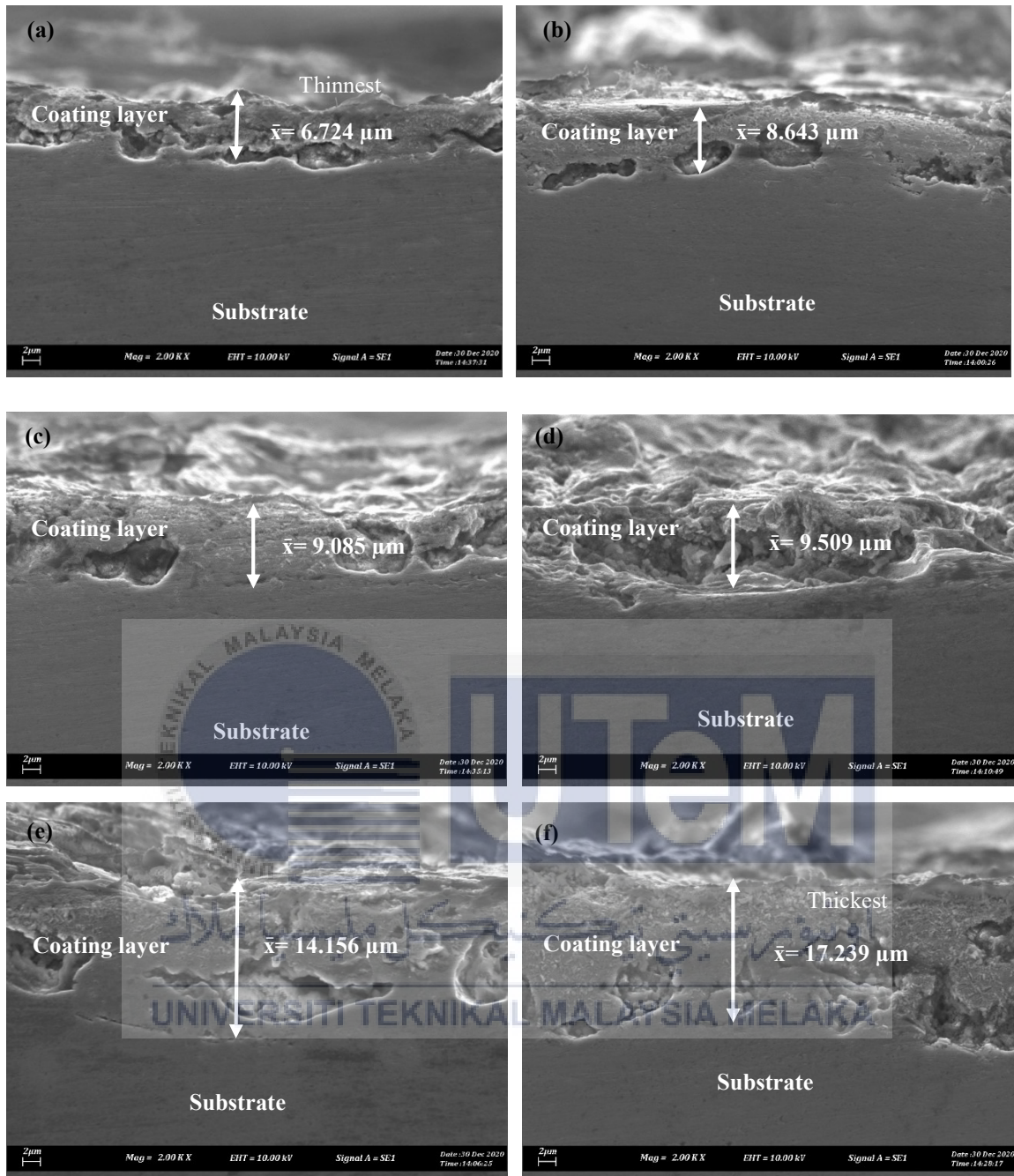
Figure 4.2: SEM image of coating layer of tungsten powder deposited on aluminium 6061
workpiece with condition (a) Ip=3A, T_{ON}=150 µs (b) Ip=3A, T_{ON}=200 µs (c) Ip=3A, T_{ON}=250 µs
(d) Ip=4A, T_{ON}=150 µs (e) Ip=4A, T_{ON}=200 µs (f) Ip=4A, T_{ON}=250 µs.

Table 4.1: Average coating thickness on aluminium 6061 workpiece.

Parameter		Average coating thickness, μm
Peak current,Ip (A)	Pulse on time,T$_{ON}$ (μs)	
3	150	6.724
	200	8.643
	250	9.085
4	150	9.509
	200	14.156
	250	17.239

4.3   Effect of Peak Current and the Thickness of Coating Layer

In this research, the parameter of peak current and pulse on time were varied. However, the setting for discharge voltage, machining time and pulse of time were remain constant at 40V, 30 minutes and 20 μs. Based on tabulated data in Table 4.1, the relationship between the effect of peak current with the thickness of coating layer was analyzed and presented in Figure 4.3.

Figure 4.3: Effect of peak current on the coating layer thickness.

From Figure 4.3, the average thickness of coating layer shows an increment as the value of peak current increases from 3A to 4A for every pulse on time. The thinnest average value 6.724 µm was observed at 3A and the thickest average value 17.239 µm was observed at parameter 4A. Generally, peak current is the most influencing factor in EDC. Peak current was described as the maximum input current that generates spark between the electrode and workpiece where the current increases over each on-time cycle until it reaches a preset level (Taylor & Das, 2012). According to Mussada and Patowari, (2015), the thickness of coating layer is significantly related with the peak current applied. Recent research by Tyagi et al. (2020) stated that, this phenomenon happened because more material is melted in the plasma channel by stronger spark that produced during the EDC process when a high peak current is applied. Therefore, a higher rate deposition of tungsten powder was observed on aluminium 6061 surface which lead to thicker coating layer as the value of peak current increases.

4.4   Effect of Pulse on Time and the Thickness of Coating Layer.

Based on tabulated data in Table 4.1, the relationship between the effect of pulse on time with the thickness of coating layer was analyzed and represented in Figure 4.4.
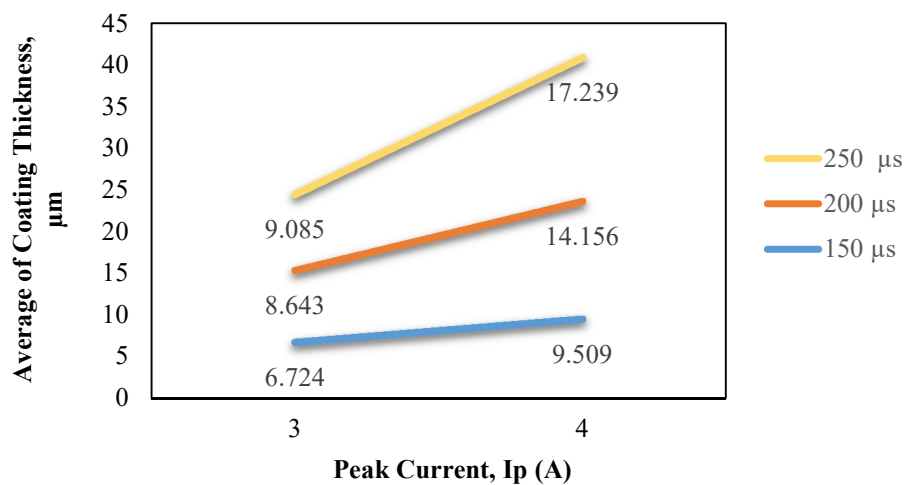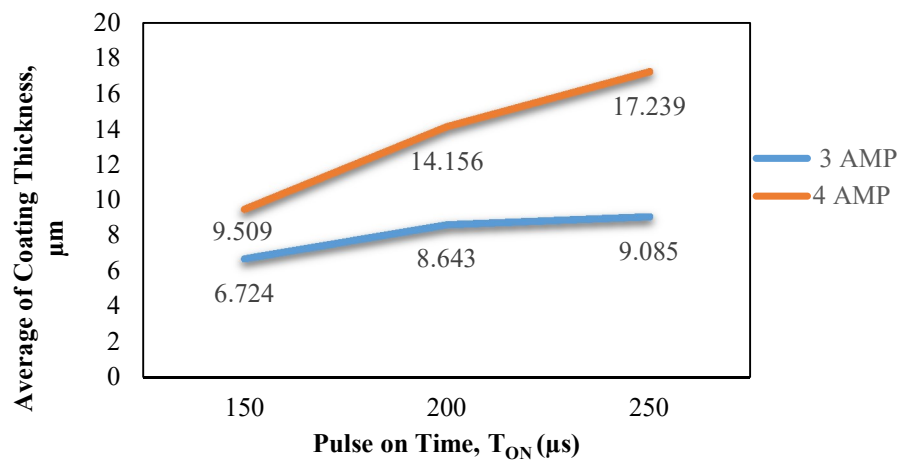

Figure 4.4: Effect of pulse on time on the coating layer thickness.

From Figure 4.4, at the peak current of 3A, the thickness of coating layer were increases from 6.724 μm to 9.396 μm as the value of pulse on time increased. The same pattern of plotted graph also can be seen at 4A of peak current where the thickness of coating layer shows an increment from 9.509 μm to 17.239 μm. Tijo and Masanta (2014) analyzed that a higher rate of deposition was observed when the value of pulse on time increases. This statement was supported by Chakraborty et al. (2018) where they explained that, during the process of electro discharge, spark is generated in between the electrode and workpiece. When longer time is applied for the pulse on time, therefore a higher volume of material will be melted and deposited on the workpiece. Elaiyarasan et al. (2018) reported that, at a low value of pulse on time, the deposition of material is lower due to the diameter of the plasma channel is small. In this situation, only a small volume of particle is present between the electrode and workpiece, resulted to a small volume of material that melted and deposited on the workpiece. However, at high value of pulse on time, the plasma channel expanded, and the volume of melted material is high.

CHAPTER 5

CONCLUSIONS AND RECOMMENDATIONS

5.1   Conclusions

In this research, surface modification of aluminium 6061 was conducted by using EDC process with W powder as a powder additive. The parameters such as peak current and pulse on time were varied to investigate the effect with the thickness of coating layer. The important findings are concluded, as below:

(a)   The W powders have an irregular shape and average size of 1.29 µm.

(b)   When the value of peak current increases, the thickness of coating layer also increased.

(c)   When the duration of pulse on time increases, the thickness of coating layer also shows an increment.

(d)   The thinnest coating layer was observed at I_p=3A and T_{ON}=150 µs with the average thickness of 6.724 µm, while the thickest coating layer was observed at parameter I_p=4A and T_{ON}=250 µs with the average coating layer thickness of 17.239 µm.

5.2   Recommendations

After this research was done, there are few recommendations that need to be focused on in future to provide more data and information in EDC process. The recommendation as follows:

(a)   Varies the parameter of powder concentration.

(b)   Wear resistance test, corrosion resistance test and surface roughness test on the coating layer are suggested to be done for coming research.

5.3   Sustainability Element
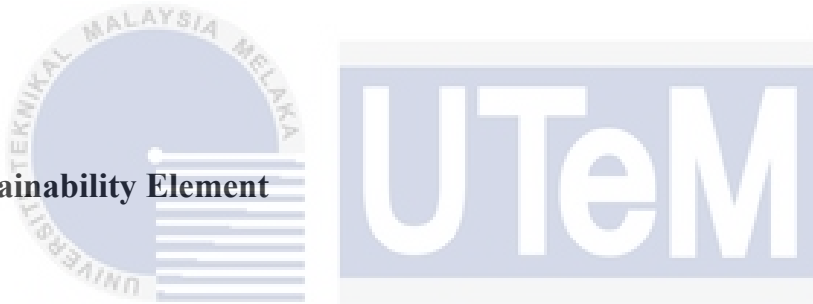
This research was motivated by the innovation of surface modification of metal by using EDC process. In sustainability, three elements are needed or also known as pillar sustainability which are environmental, social and economic development. This research will contribute to:

(a)   Compared to other coating technique, EDC use a low usage of chemical which also lead to reduction of waste material. This behaviour will protect the environment from pollution especially air and soil pollution that commonly caused by chemical disposal from industry.

(b)   From the data and result that obtained from this research, it will give many beneficiary to society, especially in the field of education and engineering. Both field commonly will seek an opportunities for improvement by applying the technique and also from continuous research and development (R&D). In

future, the usage of wasted material as a powder addition such as quarry dust and ceramic waste should be used to protect our environment and to create awareness among people.

(c)   In term of economy, the development of EDC process definitely will attract industry in future. EDC process required a low cost operation compared to another coating technique since it uses the same machine of EDM. There is no need to buy another type of machine. In the other hand, EDC also did not required a lot of process stage, this definitely will reduce operation cost and less labour cost at the same time give profit to the company.

5.4   Life Long Learning Element

For further improvement in this field of research, a lot of journal, book, article and any other sources that related should be used as a references. Commonly, research exhibition is the best platform to introduce their ideas to industry. Corporation with another universities and also industry will help in improvement of research. This improvement definitely beneficial for all organisation that involved. With the usage of EDC process and more R&D to be done, it is not possible this technique will widely use in future especially in fabrication of mold and die. When the usage of EDC coating technique penetrated world market, more profit will be gain.

5.5   Complexity Element

The complexity element of this research is to identify a suitable parameter that need to be used. Each parameter is not randomly chosen, a lot of papers or articles were used as a reference and all the parameters need to undergo try and error process. A lot of times were needed to find a suitable parameter. Next, a suitable cutting method or technique used is

important to gain the cross section of the workpiece to avoid the coating from flakes out. In the other hand, the grinding and polishing method also required a good skill, so then, less scratch can be found and easy to identify the coating layer. To confirm the existence of coating layer, Energy Dispersive X-ray (EDX) to confirm the existence of W on workpiece.
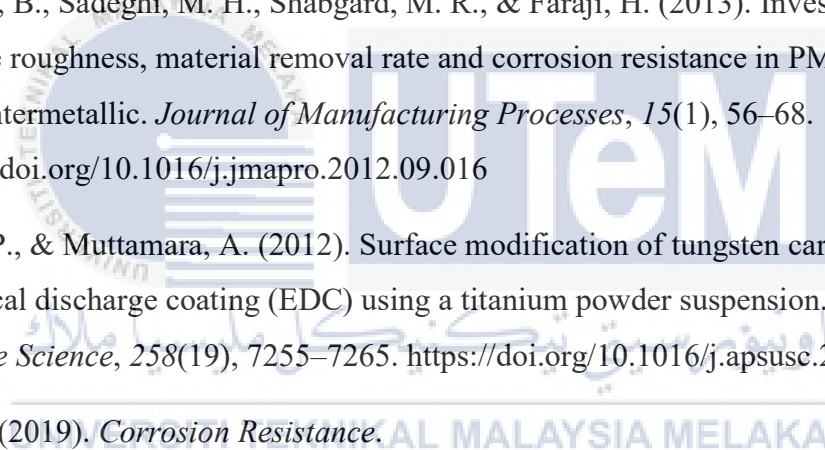
REFERENCES

Abdudeen, A., Qudeiri, J. E. A., Kareem, A., & Ahammed, T. (2020). *Recent Advances and Perceptive Insights into Powder-Mixed Dielectric Fluid of EDM*.

Akpan, I. A., & Offiong, N. A. O. (2013). Inhibition of mild steel corrosion in hydrochloric acid solution by ciprofloxacin drug. *International Journal of Corrosion*, *2013*, 1–6. https://doi.org/10.1155/2013/301689

Alcotec. (2020). *Understanding The Alloys Of Aluminum*. http://www.alcotec.com/us/en/education/knowledge/techknowledge/understanding-the-alloys-of-aluminum.cfm#

Algodi, S. J., Murray, J. W., Clare, A. T., & Brown, P. D. (2015). Characterisation of TiC layers deposited using an electrical discharge coating process. *Journal of Physics: Conference Series*, *644*(1). https://doi.org/10.1088/1742-6596/644/1/012008

Algodi, Samer J., Murray, J. W., Clare, A. T., & Brown, P. D. (2018). Modelling and Characterisation of Electrical Discharge TiC-Fe Cermet Coatings. *Procedia CIRP*, *68*(April), 28–33. https://doi.org/10.1016/j.procir.2017.12.017

Algodi, Samer J., Murray, J. W., Fay, M. W., Clare, A. T., & Brown, P. D. (2016a). Electrical discharge coating of nanostructured TiC-Fe cermets on 304 stainless steel. *Surface and Coatings Technology*, *307*, 639–649. https://doi.org/10.1016/j.surfcoat.2016.09.062

Algodi, Samer J., Murray, J. W., Fay, M. W., Clare, A. T., & Brown, P. D. (2016b). Electrical discharge coating of nanostructured TiC-Fe cermets on 304 stainless steel. *Surface and Coatings Technology*, *307*, 639–649. https://doi.org/10.1016/j.surfcoat.2016.09.062

Amorim, F. L., Dalcin, V. A., Soares, P., & Mendes, L. A. (2017). Surface modification of tool steel by electrical discharge machining with molybdenum powder mixed in dielectric fluid. *International Journal of Advanced Manufacturing Technology*, *91*(1–

4), 341–350. https://doi.org/10.1007/s00170-016-9678-x

Aydemir, B., Cal, B., Salman, S., & Salman, S. (2011). The Advantages of New Generation Hardness Measurement Methods. *5th International Quality Conference*, 337–344. http://www.cqm.rs/2011/cd/5iqc/pdf/042.pdf

Azom. (2020). *Aluminium : Specifications , Properties , Classifications*. 1–12.

Banker, K. S., PARMAR, S. P., & PAREKH, B. C. (2013). *Review to Performance Improvement of Die Sinking EDM Using Powder Mixed Dielectric Fluid*. *1*, 57–62.

Banu, A., & Ali, M. Y. (2016). Electrical Discharge Machining (EDM): A Review. *International Journal of Engineering Materials and Manufacture*, *1*(1), 3–10. https://doi.org/10.26776/ijemm.01.01.2016.02

Bojorquez, B., Marloth, R. T., & Es-Said, O. S. (2002). Formation of a crater in the workpiece on an electrical discharge machine. *Engineering Failure Analysis*, *9*(1), 93–97. https://doi.org/10.1016/S1350-6307(00)00028-5

Bui, V. D., Mwangi, J. W., & Schubert, A. (2019). Powder mixed electrical discharge machining for antibacterial coating on titanium implant surfaces. *Journal of Manufacturing Processes*, *44*(April), 261–270. https://doi.org/10.1016/j.jmapro.2019.05.032

Chakraborty, S., Kar, S., Dey, V., & Ghosh, S. K. (2018). The phenomenon of surface modification by electro-discharge coating process: A review. *Surface Review and Letters*, *25*(1), 1–12. https://doi.org/10.1142/S0218625X18300034

Chen, S. L., Lin, M. H., Huang, G. X., & Wang, C. C. (2014). Research of the recast layer on implant surface modified by micro-current electrical discharge machining using deionized water mixed with titanium powder as dielectric solvent. *Applied Surface Science*, *311*, 47–53. https://doi.org/10.1016/j.apsusc.2014.04.204

Chi, Y., Gu, G., Yu, H., & Chen, C. (2018). *Laser surface alloying on aluminum and its alloys : A review*. *100*(July 2017), 23–37. https://doi.org/10.1016/j.optlaseng.2017.07.006

Chung, D. K., Kim, B. H., & Chu, C. N. (2007). Micro electrical discharge milling using deionized water as a dielectric fluid. *Journal of Micromechanics and Microengineering*, *17*(5), 867–874. https://doi.org/10.1088/0960-1317/17/5/004

Dong, Y., & Lu, Y. (2017). Effects of Tungsten Addition on the Microstructure and Mechanical Properties of Near-Eutectic AlCoCrFeNi 2 High-Entropy Alloy. *Journal of Materials Engineering and Performance*. https://doi.org/10.1007/s11665-017-3096-6

Dvoracek, J., Sousedikova, R., Vratny, T., & Jurekova, Z. (2018). *GLOBAL TUNGSTEN DEMAND AND SUPPLY FORECAST. 62*(2017), 3–12. https://doi.org/10.1515/amsc-2017-0001

Ekmekci, B., Ulusöz, F., Ekmekci, N., & Yaşar, H. (2015). Suspended SiC particle deposition on plastic mold steel surfaces in powder-mixed electrical discharge machining. *Proceedings of the Institution of Mechanical Engineers, Part B: Journal of Engineering Manufacture*, *229*(3), 475–486. https://doi.org/10.1177/0954405414530902

Elaiyarasan*, U., Satheeshkumar, V., & Senthilkumar, C. (2018). *Experimental analysis of electrical discharge coating characteristics of magnesium alloy using response surface methodology*.

EPA. (2014). *Technical Fact Sheet – Tungsten At a Glance. January*, 1–6.

Fong, T. Y., & Chen, F. C. (2005a). Investigation into some surface characteristics of electrical discharge machined SKD-11 using powder-suspension dielectric oil. *Journal of Materials Processing Technology*, *170*(1–2), 385–391. https://doi.org/10.1016/j.jmatprotec.2005.06.006

Fong, T. Y., & Chen, F. C. (2005b). Investigation into some surface characteristics of electrical discharge machined SKD-11 using powder-suspension dielectric oil. *Journal of Materials Processing Technology*, *170*(1–2), 385–391. https://doi.org/10.1016/j.jmatprotec.2005.06.006

Fuller, J. E. (1996). Electrical Discharge Machining. *ASM Internaational*, *16*, 557–564.

Furutania, K., Saneto, A., Takezawa, H., Mohri, N., & Miyake, H. (2001). Accretion of titanium carbide by electrical discharge machining with powder suspended in working fluid. *Precision Engineering*, *25*(2), 138–144. https://doi.org/10.1016/S0141-6359(00)00068-4

Garg, R. K., Singh, K. K., Sachdeva, A., Sharma, V. S., Ojha, K., & Singh, S. (2010).

Review of research work in sinking EDM and WEDM on metal matrix composite materials. *International Journal of Advanced Manufacturing Technology*, *50*(5–8), 611–624. https://doi.org/10.1007/s00170-010-2534-5

Gregersen, E. (2020). *Tungsten*. https://www.britannica.com/science/tungsten-chemical-element

Ho, K. H., & Newman, S. T. (2003). State of the art electrical discharge machining (EDM). *International Journal of Machine Tools and Manufacture*, *43*(13), 1287–1300. https://doi.org/10.1016/S0890-6955(03)00162-7

Iqbal, M., Shaukat, I., Mahmood, A., Abbas, K., & Haq, M. A. (2010). Surface modification of mild steel with Boron Carbide reinforcement by electron beam melting. *Vacuum*, *85*(1), 45–47. https://doi.org/10.1016/j.vacuum.2010.03.009

Jabbaripour, B., Sadeghi, M. H., Shabgard, M. R., & Faraji, H. (2013). Investigating surface roughness, material removal rate and corrosion resistance in PMEDM of γ-TiAl intermetallic. *Journal of Manufacturing Processes*, *15*(1), 56–68. https://doi.org/10.1016/j.jmapro.2012.09.016

Janmanee, P., & Muttamara, A. (2012). Surface modification of tungsten carbide by electrical discharge coating (EDC) using a titanium powder suspension. *Applied Surface Science*, *258*(19), 7255–7265. https://doi.org/10.1016/j.apsusc.2012.03.054

Janssen, C. (2019). *Corrosion Resistance*.

Kalpakjian, S., Schmid, S. R., & Sekar, K. S. V. (2018). *Manufacturing Engineering and Technology* (Issue October 2013).

Kanpara, S., Govindarajan, S., Materials, N., Bhope, K., & Khirwadkar, S. (2014). *Development of Tungsten Coating using Atmospheric Plasma Spraying for First Wall Applications in Fusion TOKAMAK Development of Tungsten Coating using Atmospheric Plasma Spraying for First Wall Applications in Fusion TOKAMAK*. *November*, 2–4. https://doi.org/10.13140/2.1.4362.9120

Kansal, H. K., Singh, S., & Kumar, P. (2005). Application of Taguchi method for optimisation of powder mixed electrical discharge machining. *International Journal of Manufacturing Technology and Management*, *7*(2–4), 329–341. https://doi.org/10.1504/IJMTM.2005.006836

Kansal, H. K., Singh, S., & Kumar, P. (2007). *Technology and research developments in powder mixed electric discharge machining (PMEDM). 184*, 32–41. https://doi.org/10.1016/j.jmatprotec.2006.10.046

Karthi, S., Sivaharinathan, N., Ismai, A. M., & Elaiyarasan, U. (2018). *The coating on Al6061 Aluminium alloy surface with WC/Ni minium alloy surface with WC/Ni powder compact electrode using electrical discharge powder compact electrode using electrical discharge machining*. 872–877.

Khan, A. A., Ndaliman, M. B., Zain, Z. M., Jamaludin, M. F., & Patthi, U. (2012). Surface modification using electric discharge machining (EDM) with powder addition. *Applied Mechanics and Materials*, *110–116*(June 2014), 725–733. https://doi.org/10.4028/www.scientific.net/AMM.110-116.725

Khan, D. A., & Hameedullah, M. (2011). Effect of tool polarity on the machining characteristics in electric discharge machining of silver steel and statistical modelling of the process. *International Journal of Engineering Science …*, *3*(6), 5001–5010. http://www.ijest.info/docs/IJEST11-03-06-091.pdf

Krar, S. (2016). *ELECTRICAL DISCHARGE MACHINING (Cutting Metal to Precise Shapes using Electricity)*. 1–3.

Kumar, H., & Davim, J. P. (2011). Role of powder in the machining of Al-10%Sicp metal matrix composites by powder mixed electric discharge machining. *Journal of Composite Materials*, *45*(2), 133–151. https://doi.org/10.1177/0021998310371543

Kumar, S., & Batra, U. (2012). Surface modification of die steel materials by EDM method using tungsten powder-mixed dielectric. *Journal of Manufacturing Processes*, *14*(1), 35–40. https://doi.org/10.1016/j.jmapro.2011.09.002

Kumar, S., Singh, R., Singh, T. P., & Sethi, B. L. (2009). Surface modification by electrical discharge machining: A review. *Journal of Materials Processing Technology*, *209*(8), 3675–3687. https://doi.org/10.1016/j.jmatprotec.2008.09.032

Kumari, S. (2015). *Study of TiC coating on different type steel by electro discharge coating. 213*, 55.

Kunieda, M., Lauwers, B., Rajurkar, K. P., & Schumacher, B. M. (2005). Advancing EDM through fundamental insight into the process. *CIRP Annals - Manufacturing*

Technology, *54*(2), 64–87. https://doi.org/10.1016/s0007-8506(07)60020-1

Laparra, M. (2012). *The Aluminium False Twins. Charles Martin Hall and Paul Heroult's First Experiments and Technological Options _ Enhanced Reader.pdf* (pp. 84–105). https://www.cairn.info/revue-cahiers-d-histoire-de-l-aluminium-2012-1-page-84.htm

Li, G., Jie, X., & He, L. (2011). High temperature oxidation behavior of (Ti, Al) C ceramic coatings on carbon steel prepared by electrical discharge coating in kerosene. *Advanced Materials Research*, *189–193*, 186–192. https://doi.org/10.4028/www.scientific.net/AMR.189-193.186

Liew, P. J., Yap, C. Y., Nurlishafiqa, Z., Othman, I. S., Chang, S. Y., Toibah, A. R., & Wang, J. (2018). Material deposition on aluminium by Electrical discharge coating (Edc) with a tungsten powder suspension. *Journal of Advanced Manufacturing Technology*, *12*(2), 133–145.

Liew, Pay Jun, Yan, J., & Kuriyagawa, T. (2013). Experimental investigation on material migration phenomena in micro-EDM of reaction-bonded silicon carbide. *Applied Surface Science*, *276*, 731–743. https://doi.org/10.1016/j.apsusc.2013.03.161

Liew, Pay Jun, Yap, C. Y., Wang, J., Zhou, T., & Yan, J. (2020). Surface Modification and Functionalization by Electrical Discharge Coating - A Comprehensive Review. *International Journal of Extreme Manufacturing*. https://doi.org/10.1088/2631-7990/ab7332

Mahendran, S., Devarajan, R., Nagarajan, T., & Majdi, A. (2010). *A Review of Micro-EDM*. June 2014.

Marashi, H., Jafarlou, D. M., Sarhan, A. A. D., & Hamdi, M. (2016). State of the art in powder mixed dielectric for EDM applications. *Precision Engineering*, *46*, 11–33. https://doi.org/10.1016/j.precisioneng.2016.05.010

Matmatch. (2020). *Properties of tungsten*. https://matmatch.com/learn/material/tungsten

Mazarbhuiya, R. M., Dutta, H., Debnath, K., & Rahang, M. (2020). Surface modification of CFRP composite using reverse-EDM method. *Surfaces and Interfaces*, *18*. https://doi.org/10.1016/j.surfin.2020.100457

McDonnell, B. (2010). Jesters to the revolution - A history of Cartoon Archetypical Slogan Theatre (CAST), 1965 - 85. *Theatre Notebook*, *64*(2), 96–111.

Murray, J. W., Algodi, S. J., Fay, M. W., Brown, P. D., & Clare, A. T. (2017). Formation mechanism of electrical discharge TiC-Fe composite coatings. *Journal of Materials Processing Technology*, *243*, 143–151. https://doi.org/10.1016/j.jmatprotec.2016.12.011

Murray, James W., & Clare, A. T. (2016). Morphology and Wear Behaviour of Single and Multi-layer Electrical Discharge Coatings. *Procedia CIRP*, *42*(Isem Xviii), 236–239. https://doi.org/10.1016/j.procir.2016.02.278

Mussada, E. K., & Patowari, P. K. (2015a). Characterisation of layer deposited by electric discharge coating process. *Surface Engineering*, *31*(10), 796–802. https://doi.org/10.1179/1743294415Y.0000000048

Mussada, E. K., & Patowari, P. K. (2015b). Characterisation of layer deposited by electric discharge coating process. *Surface Engineering*, *31*(10), 796–802. https://doi.org/10.1179/1743294415Y.0000000048

Nanimina, A. M., Abdul Rani, A. M., & Ginta, T. L. (2014). Assessment of Powder Mixed EDM: A Review. *MATEC Web of Conferences*, *13*, 04018. https://doi.org/10.1051/matecconf/20141304018

Niinomi, M., Liu, Y., Nakai, M., Liu, H., & Li, H. (2016). *Biomedical titanium alloys with Young ' s moduli close to that of cortical bone. March*, 173–185. https://doi.org/10.1093/rb/rbw016

Nunes, R., Ammons, M., Avery, H. S., Bean, J. C., Berry, D. F., & Blackmon, C. M. (1990). *The Materials Information Company*. ASM INTERNATIONAL HANDBOOK.

Olsen, D. (2020a). *Welcome to the MetalTek Blog . Material Applications : Corrosion Resistance*. 1–5.

Olsen, D. (2020b). *Why Certain Metals Offer Greater Wear Resistance*. 4–7.

Oshida, Y. (2013). Surface Modifications. In *Bioscience and Bioengineering of Titanium Materials*. https://doi.org/10.1016/b978-0-444-62625-7.00011-x

Panda, B. K. (2019). Impact of Powder-mixed Electrical Discharge Machining on Surface Hardness of AISI D3 Die Steel. *2019 IEEE 10th International Conference on Mechanical and Aerospace Engineering (ICMAE)*, 218–222.

Patowari, P. K., & Mussada, E. K. (2017). Post processing of the layer deposited by electric discharge coating. *Materials and Manufacturing Processes*, *32*(4), 442–449. https://doi.org/10.1080/10426914.2016.1198021

Patowari, P. K., Saha, P., & Mishra, P. K. (2015). An experimental investigation of surface modification of C-40 steel using W–Cu powder metallurgy sintered compact tools in EDM. *International Journal of Advanced Manufacturing Technology*, *80*(1–4), 343–360. https://doi.org/10.1007/s00170-015-7004-7

Prakash, C., Kansal, H. K., Pabla, B. S., & Puri, S. (2015). Processing and Characterization of Novel Biomimetic Nanoporous Bioceramic Surface on β-Ti Implant by Powder Mixed Electric Discharge Machining. *Journal of Materials Engineering and Performance*, *24*(9), 3622–3633. https://doi.org/10.1007/s11665-015-1619-6

Prakash, C., Kansal, H. K., Pabla, B. S., & Puri, S. (2017). Experimental investigations in powder mixed electric discharge machining of Ti–35Nb–7Ta–5Zrβ-titanium alloy. *Materials and Manufacturing Processes*, *32*(3), 274–285. https://doi.org/10.1080/10426914.2016.1198018

Prakash, C., Kansal, H. K., & Puri, S. (2015). *Potential of Powder Mixed Electric Discharge Machining to Enhance the Wear and Tribological Performance of β -Ti Implant for Orthopedic Applications. September 2016*. https://doi.org/10.1166/jnan.2015.1245

Prakash, C., & Uddin, M. S. (2017). Surface modification of β-phase Ti implant by hydroaxyapatite mixed electric discharge machining to enhance the corrosion resistance and in-vitro bioactivity. *Surface and Coatings Technology*, *326*, 134–145. https://doi.org/10.1016/j.surfcoat.2017.07.040

Prakash, V., Shubham, Kumar, P., Singh, P. K., Das, A. K., Chattopadhyaya, S., Mandal, A., & Dixit, A. R. (2018). Surface alloying of miniature components by micro-electrical discharge process. *Materials and Manufacturing Processes*, *33*(10), 1051–1061. https://doi.org/10.1080/10426914.2017.1364755

Radu, S., Buzatu, M., & Geanta, V. (2019). *Influence of the Tungsten Content on the Elastic Modulus of New Ti-15Mo-W Alloys Intended for Medical Applications. 71*(7), 2272–2279. https://doi.org/10.1007/s11837-019-03512-w

Rahang, M., & Patowari, P. K. (2016). Parametric Optimization for Selective Surface

Modification in EDM Using Taguchi Analysis. *Materials and Manufacturing Processes*, *31*(4), 422–431. https://doi.org/10.1080/10426914.2015.1037921

Ramabalan, J. J. and S. (2015). Die Sinking Edm Process Parameters: a Review. *International Journal of Engineering and Robotics Research*, *4*(1).

Richhariya, V. (2013). *Surface Modification of AISI 1020 Mild Steel by Electrical Discharge Coating with Tungsten and Copper Mixed Powder Green Compact Electrodes Vipin Richhariya Surface Modification of AISI 1020 Mild Steel by Electrical*. 1–53.

Rodriguez, P., Caussat, B., Ablitzer, C., Iltis, X., & Brothier, M. (2011). *Alumina Coating on Dense Tungsten Powder by Fluidized Bed Metal Organic Alumina Coating on Dense Tungsten Powder by Fluidized Bed Metal Organic Chemical Vapour Deposition*. *September*. https://doi.org/10.1166/jnn.2011.5097

Sahu, A. K., & Mahapatra, S. S. (2018). *Electrical Discharge Coating by Copper-Tungsten Composite Electrode Prepared by Powder Metallurgy Route* (pp. 195–224). https://doi.org/10.4018/978-1-5225-3035-0.ch010

Sanjeev Sharma, Rajdeep Singh, & Sandeep Jindal. (2015). Study the Effect of Machining Parameters in Electric Discharge Machining of EN 31 Die Steel. *International Journal of Engineering Research And*, *V4*(11), 145–148. https://doi.org/10.17577/ijertv4is110031

Sharma, D., Mohanty, S., & Das, A. K. (2020a). Surface modification of titanium alloy using hBN powder mixed dielectric through micro-electric discharge machining. *Surface and Coatings Technology*, *381*(May 2019), 125157. https://doi.org/10.1016/j.surfcoat.2019.125157

Sharma, D., Mohanty, S., & Das, A. K. (2020b). Surface modification of titanium alloy using hBN powder mixed dielectric through micro-electric discharge machining. *Surface and Coatings Technology*, *381*, 125157. https://doi.org/10.1016/j.surfcoat.2019.125157

Shibe, V., & Chawla, V. (2014). A Review of Surface Modification Techniques in Enhancing the Erosion Resistance of Engineering Components. *International Journal of Research in Mechanical Engineering & Technology*, *4*(2), 2249–5762.

Singh, S., & Bhardwaj, A. (2011). Review to EDM by Using Water and Powder-Mixed Dielectric Fluid. *Journal of Minerals and Materials Characterization and Engineering*, *10*(02), 199–230. https://doi.org/10.4236/jmmce.2011.102014

Stojanovic, B., Bukvic, M., & Epler, I. (2018). *Application of Aluminum and Aluminum Alloys in Engineering. October*. https://doi.org/10.18485/aeletters.2018.3.2.2

Sumi, N., GOTO, A., TERAMOTO, H., YASUNAGA, Y., & NAKANO, Y. (2011). Study of Si-containing amorphous layer by electrical discharge coating. *International Journal of Electrical Machining*, *16*(0), 27–32. https://doi.org/10.2526/ijem.16.27

Sumi, N., GOTO, A., TERAMOTO, H., YASUNAGA, Y., & NAKANO, Y. (2012). Study of improvement of TiC layer by electrical discharge coating. *Journal of The Japan Society of Electrical Machining Engineers*, *46*(113), 133–140. https://doi.org/10.2526/jseme.46.133

Surekha, B., Gangadhara Rao, P., Bijetha, B., & Srinivasa Sai, V. (2018). Surface characteristics of EN19 steel materials by EDM using Graphite mixed Dielectric medium. *Materials Today: Proceedings*, *5*(9), 17895–17900. https://doi.org/10.1016/j.matpr.2018.06.117

Talla, G. (2016). *Powder-mixed Electric Discharge Machining (PMEDM) of Inconel 625 Powder-mixed Electric Discharge Machining (PMEDM) of Inconel 625*.

Taylor, P., & Das, A. (2012). *Machining Science and Technology : An EXPERIMENTAL INVESTIGATION ON SURFACE MODIFICATION OF ALUMINUM BY ELECTRIC DISCHARGE COATING PROCESS USING TiC / Cu GREEN COMPACT. February 2013*, 37–41. https://doi.org/10.1080/10910344.2012.731951

Teimouri, R., & Baseri, H. (2012). Study of tool wear and overcut in EDM process with rotary tool and magnetic field. *Advances in Tribology*, *2012*. https://doi.org/10.1155/2012/895918

Tijo, D., & Masanta, M. (2014). Surface modification of aluminum by electrical discharge coating with tungsten and copper mixed powder green compact electrodes. *5th International & 26th All India Manufacturing Technology, Design and Research Conference*, *Aimtdr*, 190. https://doi.org/10.13140/2.1.2896.4648

Tijo, D., & Masanta, M. (2017). Mechanical performance of in-situ TiC-TiB2 composite

coating deposited on Ti-6Al-4V alloy by powder suspension electro-discharge coating process. *Surface and Coatings Technology*, *328*, 192–203. https://doi.org/10.1016/j.surfcoat.2017.08.048

Toshimitsu, R., Okada, A., Kitada, R., & Okamoto, Y. (2016). Improvement in Surface Characteristics by EDM with Chromium Powder Mixed Fluid. *Procedia CIRP*, *42*(Isem Xviii), 231–235. https://doi.org/10.1016/j.procir.2016.02.277

Tyagi, R., Das, A. K., & Mandal, A. (2018). Electrical discharge coating using WS2 and Cu powder mixture for solid lubrication and enhanced tribological performance. *Tribology International*, *120*, 80–92. https://doi.org/10.1016/j.triboint.2017.12.023

Tyagi, Rashi, Mahto, N. K., Das, A. K., & Mandal, A. (2020). Preparation of MoS2+Cu coating through the EDC process and its analysis. *Surface Engineering*, *36*(1), 86–93. https://doi.org/10.1080/02670844.2019.1615744

Tzeng, Y. F., & Lee, C. Y. (2001). Effects of powder characteristics on electrodischarge machining efficiency. *International Journal of Advanced Manufacturing Technology*, *17*(8), 586–592. https://doi.org/10.1007/s001700170142

Ueno, M., Fujita, N., Kimura, Y., & Nakata, N. (2016). Evaluation of coating and wear characteristics of roll surface coated with TiC by electrical discharge coating. *Journal of Materials Processing Technology*, *236*, 9–15. https://doi.org/10.1016/j.jmatprotec.2016.04.025

Vargel, C. (2004). corrosion of aluminium. *Journals Ofalloys and Compunds*.

Verdins, G., Kanaska, D., & Kleinbergs, V. (2013). Selection of the method of hardness test. *Engineering for Rural Development*, 217–222.

Watane, K. (2017). International Engineering Journal For Research & Development ENHANCEMENT OF SURFACE HARDNESS OF MILD STEEL BY International Engineering Journal For Research & Development. *ENHANCEMENT OF SURFACE HARDNESS OF MILD STEEL BY USING EDC*, *4*(7), 1–6.

Woodford, C. (2020). *What's aluminum like?* (Issue Mmc, pp. 1–7). https://www.explainthatstuff.com/aluminum.html

Zain, Z. M., Ndaliman, M. B., Khan, A. A., & Ali, M. Y. (2014). Improving micro-hardness of stainless steel through powder-mixed electrical discharge machining.

Proceedings of the Institution of Mechanical Engineers, Part C: Journal of Mechanical Engineering Science, *228*(18), 3374–3380. https://doi.org/10.1177/0954406214530872

Zhu, H., Tong, H., Cheng, C., & Liu, N. (2017). Int . Journal of Refractory Metals and Hard Materials Study on behaviors of tungsten powders in radio frequency thermal plasma. *International Journal of Refractory Metals and Hard Materials*, *66*, 76–82. https://doi.org/10.1016/j.ijrmhm.2017.01.017

APPENDICES

A) Gantt chart for PSM 1

No	Task	Week 1	2	3	4	5	6	7	8	9	10	11	12	13	14
1	PSM 1 Title Selection	■													
2	Registration of PSM 1 Title	■													
	Endorsement of PSM 1 Title		■												
	Chapter 1 (Introduction)			■											
	Chapter 2 (Literature Review)				■	■	■	■							
	Chapter 2 Submission (Ulearn)											■			
	Chapter 3 (Methodology)									■	■				
3	Chapter 3 Submission (Ulearn)											■			
3	Video Preparation											■	■		
4	Video Presentation (video link)													■	
5	Completing Report and Formatting			■	■	■	■	■	■	■	■	■	■	■	■
7	Submission of PSM 1 report														■

B) Gantt chart for PSM 2

No	Task	Week														
		1	2	3	4	5	6	7	8	9	10	11	12	13	14	15
1	General briefing	■														
2	Lecture series-															
	(a) FYP 2 briefing	■														
	(b) Safety awareness			■												
	(c) Chapter 4&5 (Result, discussion, conclusion and recommendation)				■											
	(d) English Technical Talk					■										
	(e) Reference and formatting											■				
3	Run an Experiment						■	■	■	■	■		■			
4	Submission of logbook											■				
5	Video presentation (video link)													■	■	
6	Question and Answer session														■	
7	Submission of FYP report															■

C) Measurement and surface morphology of W powder
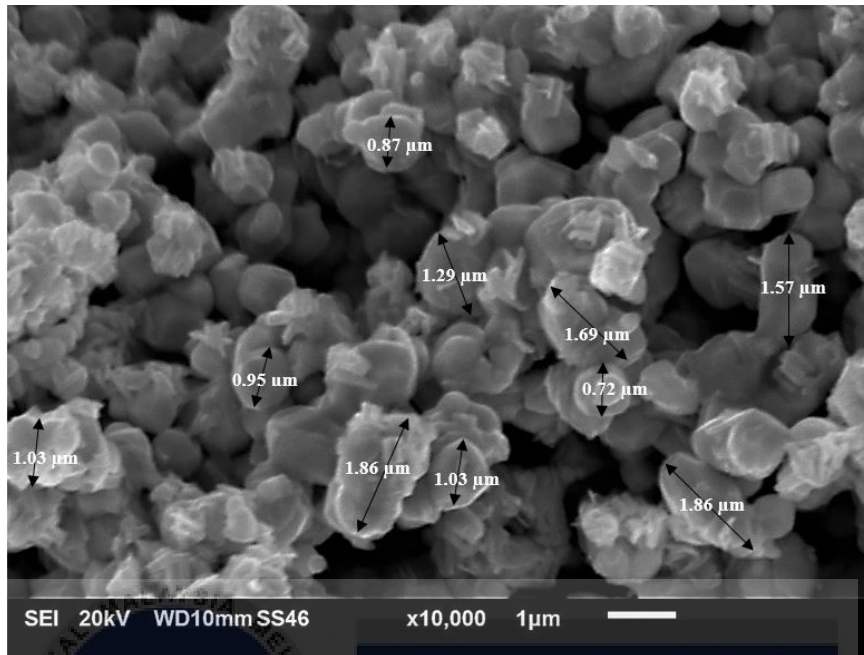
x̄ = (1.03 + 0.95 + 1.86 + 1.03 + 1.86 +0.716 + 1.69 + 1.29 + 0.87 + 1.57) μm
_____

10

x̄ = 1.29 μm

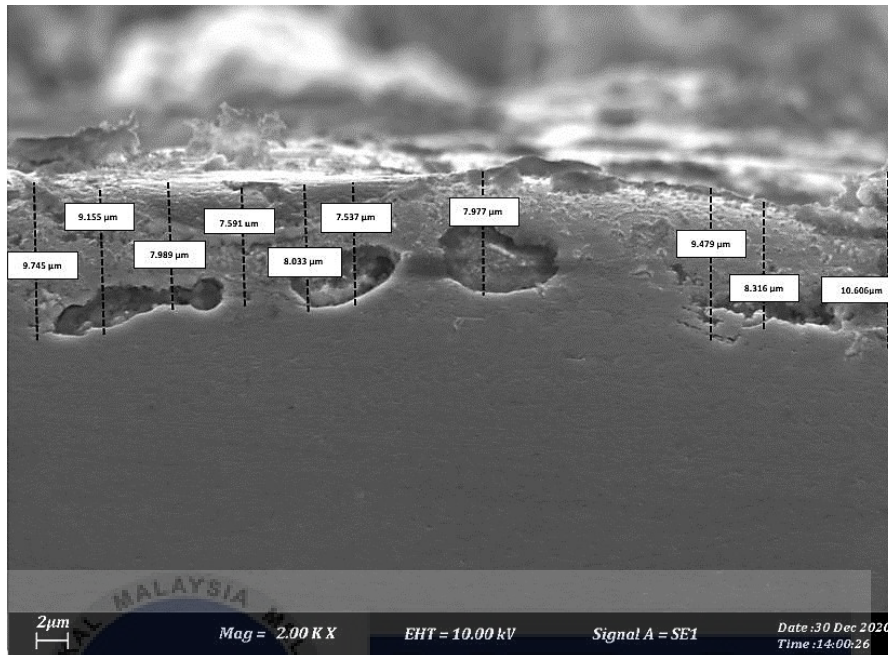**D) Measurement and average of coating layer thickness.**

    i.   **Ip = 3A, T$_{ON}$ = 150 μs**

$\bar{x} = \dfrac{(6.565 + 5.973 + 6.758 + 5.434 + 8.151 + 5.914 + 6.606 + 7.984 + 6.820 + 7.032)\ \mu m}{10}$

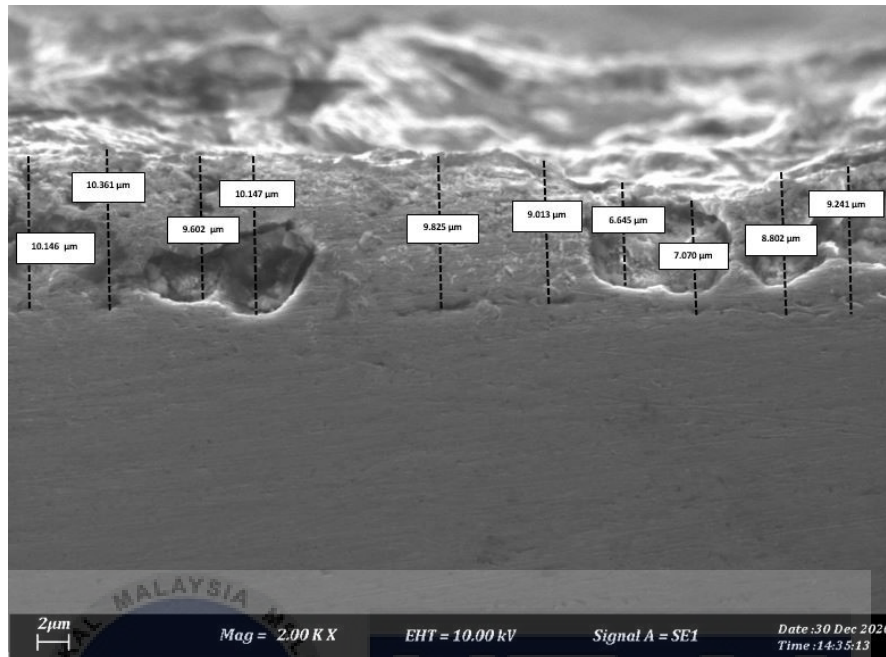$\bar{x} = 6.723\ \mu m$

ii. $I_p = 3A$, $T_{ON} = 200 \mu s$

$$\bar{x} = \frac{(9.745 + 9.155 + 7.989 + 7.591 + 8.033 + 7.537 + 7.977 + 9.479 + 8.316 + 10.606) \mu m}{10}$$

$\bar{x} = 8.643 \mu m$

iii.   Ip = 3A, T$_{ON}$ = 250 μs

$$\bar{x} = \frac{(10.146 + 10.361 + 9.602 + 10.147 + 9.825 + 9.013 + 6.645 + 7.070 + 8.802 + 9.241) \ \mu m}{10}$$

$\bar{x}$ = 9.085 μm

iv.   Ip = 4A, TON = 150 µs
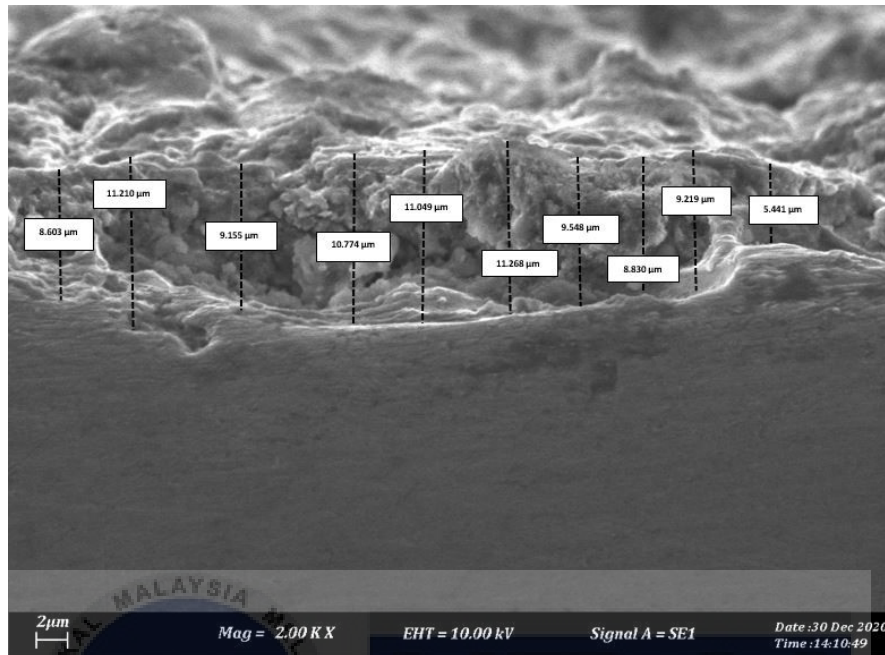
$$\bar{x} = \frac{(8.603 + 11.210 + 9.155 + 10.774 + 11.049 + 11.268 + 9.548 + 8.830 + 9.219 + 5.441) \ \mu m}{10}$$

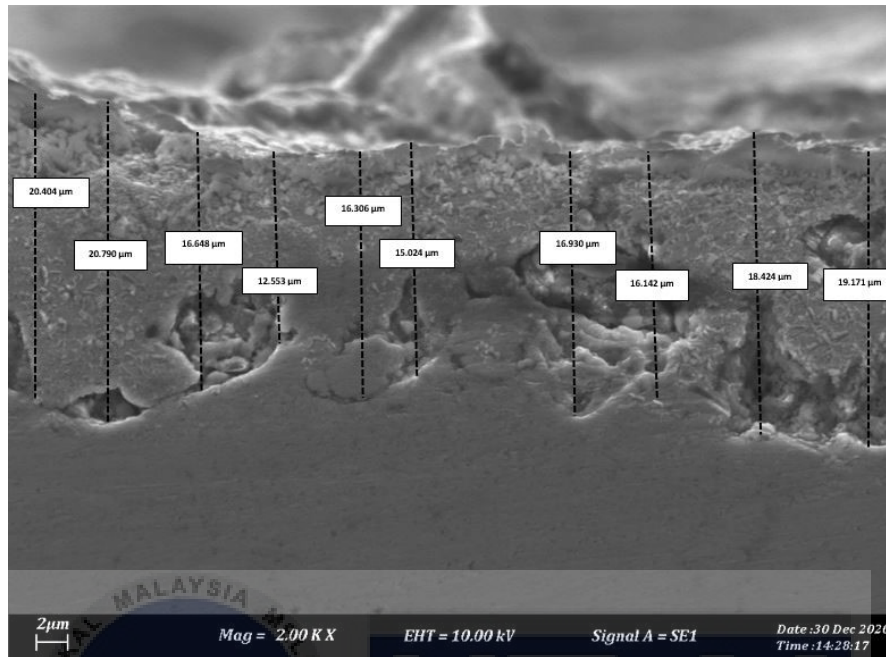$\bar{x} = 9.509 \ \mu m$

v.   Ip = 4A, TON = 200 µs
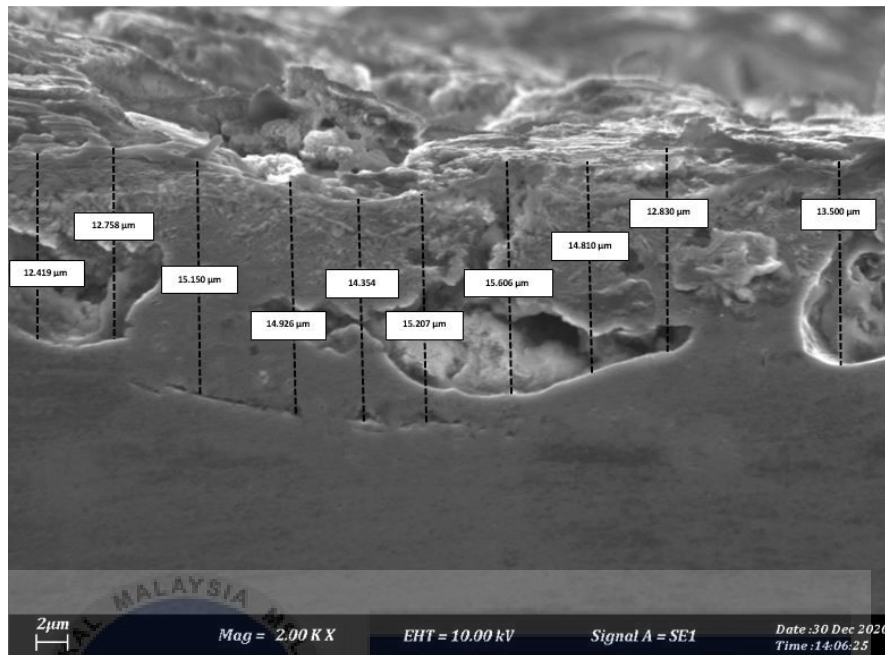
$$\bar{x} = \frac{(12.419 + 12.758 + 15.150 + 14.926 + 14.354 + 15.207 + 15.606 + 14.810 + 12.830 + 13.5) \text{ µm}}{10}$$

$\bar{x}$ = 14.156 µm

vi.   **Ip = 4A, TON = 250 μs**

$$\bar{x} = \frac{(20.404 + 20.79 + 16.648 + 12.553 + 16.306 + 15.024 + 16.93 + 16.142 + 18.424 + 19.171) \ \mu m}{10}$$

$\bar{x} = 17.239 \ \mu m$